Numerical Investigation of Overburden Failure Mechanisms and Structural Evolution in Partial Gob-Backfilling Mining of Steeply Inclined Coal Seams

Wenyu Lv, Jinghui Wang*, Chao Lyu, Yongping Wu, Panshi Xie, Xuyan He, Kai Guo and Ru You

School of Energy Engineering, Xi'an University of Science and Technology, Xi'an, China

INFORMATION

Keywords:
Steeply inclined coal seam
partial gob backfilling
overlying strata migration
ground pressure manifestation
numerical simulation

DOI: 10.23967/j.rimni.2026.10.77102

SCIPEDIA Revista Internacional de Métodos Numéricos para Cálculo y Diseño en Ingeniería

Revista Internacional Métodos numéricos para cálculo y diseño en ingeniería RIMNI in cooperation with CIMNE

Numerical Investigation of Overburden Failure Mechanisms and Structural Evolution in Partial Gob-Backfilling Mining of Steeply Inclined Coal Seams

Wenyu Lv, Jinghui Wang*, Chao Lyu, Yongping Wu, Panshi Xie, Xuyan He, Kai Guo and Ru You

School of Energy Engineering, Xi'an University of Science and Technology, Xi'an, China

ABSTRACT

In managing strong roof loading in steep-inclined longwall panels, this study adopts partial gob backfill mining along the dip direction. Four controlling factors for roof deformation are identified: working face length (L), mining depth (H), seam dip angle (α), and backfill length (a). Parametric analysis determines that L = 105 m combined with a 2/5 backfill ratio achieves optimal strata control. Physical experiments recorded dip-direction stress gradients: upper (8.65/7.79/8.45 MPa), central peak (9.86/9.15/9.86 MPa), and lower (8.82/8.41/8.83 MPa), with displacement increments of horizontal (+115.6%/+73.9%/+74.1%), vertical (+136.2%/+48.9%/+21.3%), and resultant (+80.6%/+94.8%/+39.2%). FLAC3D simulations systematically varied backfill ratios (1/5, 2/5, 3/5) and face lengths (90, 105, 120 m). Increasing the ratio from 1/5 to 2/5 reduced peak stress by 7.7% (15.65 → 14.45 MPa) and subsidence by 39.3% (1.78 → 1.08 m), while further increase to 3/5 yielded marginal gains (4.5%, 31.5%). At the optimal 2/5 ratio, extending face length from 90 to 105 m increased abutment stress by 8.9% (13.27 → 14.45 MPa) and subsidence by 17.4% (0.92 → 1.08 m), while 120 m caused disproportionate surges (5.2%, 49.1%) with plastic zone height soaring 81.9% (36.05 → 65.56 m). Under the optimal 105 m–2/5 configuration, staged advance (20–80 m) quantified progressive stress transfer: lower-end pillar stress rose 20.4% (9.22 → 11.10 MPa), backfill stress 24.7% (8.75 → 10.91 MPa), and roof subsidence from 302 to 688 mm, with plastic zone evolving as an asymmetric arch characterized by shear failure at the arch foot (lower pillar/backfill interface) and tensile failure at the crown. This integrated approach confirms that partial backfill effectively regulates strata behavior, providing a quantitative framework for sustainable steep-seam mining.

OPEN ACCESS

Received: 02/12/2025

Accepted: 18/02/2026

Published: 16/04/2026

DOI
10.23967/j.rimni.2026.10.77102

Keywords:
Steeply inclined coal seam
partial gob backfilling
overlying strata migration
ground pressure manifestation
numerical simulation

1 Introduction

The extraction of coal resources has positioned resource recovery and associated research under complex mining conditions as a primary focus in contemporary mining scholarship [1,2]. Steeply dipping coal seams are defined as coal deposits with buried dip angles ranging from 35°–55°, and are

*Correspondence: Jinghui Wang (13087671357@163.com).

internationally recognized by the mining community as complex mining environments [3]. Extensive field practices, experimental studies, and theoretical analyses demonstrate that effective control of stope surrounding rock stability constitutes the central determinant for safe and efficient mining in steeply dipping coal seams [4,5]. In longwall mining of steeply dipping coal seams, dip-directional non-uniform backfilling of gob gangue induces intensified movement of upper-middle roof strata, triggering stability failure in the roof-support system [6]. Compared with the conventional caving method, the backfill mining method establishes a dynamic support structure through front coal mass support and rear backfill support in the stope. This approach demonstrates superior effectiveness in controlling surrounding rock disasters and enhancing support stability [7–9]. Thus, studies on backfill mining applications for steep-dipping coal deposits employing longwall systems are fundamentally necessary.

Research findings during the process of coal mining, there is a violent appearance of mining stress when the initial weighting occurs [10]. Concerning strata pressure behavior, research confirms that dip-oriented longwall faces in steep coal seams display dynamic pressure redistribution over time, showing clear zonal characteristics of "initial central zone activation, followed by upper section, then lower section" [11,12]. Concerning surrounding rock failure, investigations have systematically examined roof deformation characteristics, failure mechanisms, movement patterns, and post-mining rock mass structures [13–16]. Research findings indicate distinct spatiotemporal evolution and asymmetrical characteristics in the kinematics of the immediate roof, main roof, and overburden. Concurrently, strategic coal pillar retention combined with strip backfilling demonstrates efficacy in regulating surrounding rock deformation and stress redistribution [17,18]. Studies have investigated the mechanisms of equipment sliding, tilting, and associated surrounding rock disasters [19–21]. The research indicates that in steep coal seams, immediate roof caving typically rolls and fills the lower dip area, creating an asymmetric backfilling effect. Within the midface and upper zones of the working face, the interaction between roof strata and hydraulic supports demonstrates complexity in mechanical responses, resulting in particularly demanding stability management for the support and surrounding rock structure. Notably, floor failure under such mining conditions demonstrates dip-directional asymmetry, characterized by convergent deformation in upper sections and extensional deformation in lower zones [22]. The degree of structural asymmetry shows a positive correlation with coal seam dip angles. Building upon these research findings, scholars have proposed disaster prevention and control technologies applicable to steeply dipping coal seam mining, including roof-cutting pressure relief [23], gob-side entry retaining [24], subsurface mining layouts can be optimized through geophysical survey analysis of mine structures [25], backfill mining efficacy is assessed via predictive methods for surface deformation and analogous metrics [26], nonlinear support arrangement, and zonal control of support resistance [27].

To control the stability of surrounding rock in steeply inclined coal seam stopes, researchers have proposed partial backfilling as a method to modulate the mechanical behavior in disaster-prone zones induced by structural changes of rock masses [28]. Research has demonstrated that partial backfill bodies can effectively maintain rock mass structural stability by constraining the evolution paths of surrounding rock "key zones". Prior research applied material mechanics theory to establish a mechanical model of partially backfilled roof rock beams, identifying critical backfill influencing factors while investigating roof fracture locations and associated disaster mechanisms. Subsequent investigations further developed a dip-direction mechanical model for main roof behavior under partial gangue backfill in steeply dipping coal seams, determining fracture positions and elucidating roof failure mechanisms [29]. While triaxial compression studies reveal progressive strength degradation in thermally stressed granite through microcrack coalescence [30], and adsorption models quantify

gas-induced coal matrix swelling that exacerbates fracture propagation [31], this work establishes a novel backfill-induced stress redistribution framework that actively counters such failure mechanisms by optimizing load-transfer pathways in steeply inclined seams.

Previous investigations into longwall fully mechanized extraction within steeply inclined coal seams have generated significant findings on strata movement and strata pressure manifestation patterns. Researchers developed a structural model for immediate roof beams. These outcomes substantially enhance methodologies applicable to steep coal seams, while providing deeper insights into roof failure mechanisms. However, investigations into the evolutionary behavior of overburden strata in steeply dipping strike longwall partial backfill mining, as well as the impact of partial backfill on stope surrounding rock stability, remains limited. Therefore, this study investigates the composite bearing structure of support-surrounding rock-backfill in steeply dipping stopes. Theoretical investigations yielded an analytical framework for roof beam mechanics, revealing the influencing factors and interaction mechanisms governing roof deformation and failure. Subsequently, physical similarity simulation experiments were conducted to analyze the movement evolution patterns of overlying strata under partial backfill in steeply dipping strike longwall mining, elucidating the control mechanisms of partial backfill technology on working face surrounding rock stability. Finally, numerical simulations were employed to verify and supplement the experimental results, deepening theoretical understanding of overlying strata dynamic responses and surrounding rock control mechanisms. Building upon existing research on strata behavior, surrounding rock failure, and backfill control in steeply dipping coal seam mining, this study further focuses on the entire evolution process of asymmetric deformation and stress-arch shell structures in the overburden under the specific process of partial waste rock backfilling. Compared with most studies that emphasize single approaches such as theoretical analysis, numerical simulation, or field observation, this research combines theoretical modeling, three-dimensional physical similarity experiments, and FLAC3D numerical simulation to systematically reveal the dynamic response chain from roof fracturing to stress-arch shell formation. It also clarifies the synergistic effect of the specific parameter combination—a working face length of 105 m and a backfill ratio of 2/5—in controlling asymmetric deformation of the overburden and optimizing stress distribution. The results not only verify the positive impact of partial backfill on surrounding rock stability but also provide quantitative evidence for key engineering parameters under this process from the perspective of multi-method cross-validation, offering more systematic and actionable references for field design and disaster prevention under similar conditions.

2 Deformation and Failure Mechanisms of Roof Strata under Partial Backfill

2.1 Mechanical Analysis of Roof Rock Beams

Relative to conventional caving methods, the partial backfilling approach applied to steep coal seams forms a composite "support-surrounding rock-backfill" load-bearing system, leading to distinct variations in both the stress distribution patterns within overburden strata and the evolutionary characteristics of deformation and failure. These variations are primarily reflected in the dynamic mechanical interactions between backfill materials and surrounding rock mass, as well as their asymmetric instability behaviors. The roof strata are predominantly influenced by the combined effects of overburden gravity and backfill support forces. According to these mechanical characteristics, a unit-width roof beam model along the face dip direction is established for analysis, developing a structural mechanics framework for inclined roof strata in steep coal seams with partial backfill conditions (Fig. 1). The key parameters are defined as follows: α denotes the coal seam dip angle; L represents the working face length; h indicates the roof beam thickness; a and b correspond to the lengths of backfilled section AB and unfilled section BC, respectively; F_c and M_c refer to the constraint

force and bending moment at point C; while R_A and R_C signify the reaction forces at points A and C of the roof beam ($R_A = R_C$).

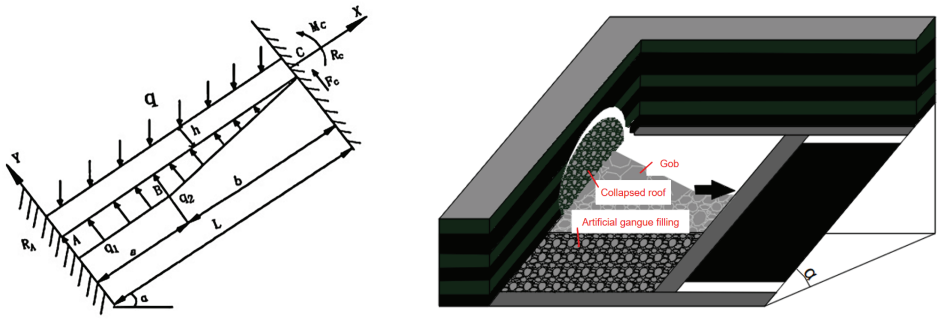

(**a**) (**b**)

Figure 1: Schematic representation of strata response to partial backfill in steep coal seams. (a) Schematic diagram of mechanical structure; (b) Conceptual diagram of downhole partial filling

The roof beam sustains a constant pressure exerted by superincumbent strata:

$$q = \gamma H \tag{1}$$

with γ representing the bulk density of superincumbent strata and H denoting the extraction depth.

Due to the mutual supporting interaction between backfill and surrounding rock, the load on roof section AB is uniformly distributed over the backfill, expressed as $q_1 = kq\cos\alpha$, where k denotes the compaction rate of backfill material. In contrast, the supporting load in immediate roof caving section BC exhibits a linear distribution pattern, with $q_2 = q_1$.

Considering the mining depth substantially surpasses the roof beam thickness, the beam's self-weight is disregarded when computing dip-direction displacement at arbitrary beam locations. The displacement is given by:

$$\Delta l = \int_0^L \frac{[R_A + R_C - q\,(L-x)\sin\alpha]\,dx}{EA} = 0 \tag{2}$$

with E denoting the Young's modulus of the roof beam and A representing its sectional area.

By solving Eq. (1), the support reactions at both ends of the roof rock beam are obtained as:

$$R_A = R_c = \frac{1}{2}qL\sin\alpha \tag{3}$$

Based on the mechanical model and bending moment theory in mechanics of materials, the differential equations governing the deflection curves of sections AB and BC in the roof rock beam are derived as [32]:

$$\begin{aligned} y_{AB}{}''(x) &= \frac{M_c}{EI} + \frac{F_c}{EI}(L-x) - \frac{S}{EI}y_{AB}(x) - \frac{q\cos\alpha}{2EI}(L-x)^2 + \frac{kq\cos\alpha}{2EI}(a-x)^2 + \frac{kqb\cos\alpha}{2EI}\left(a-x+\frac{b}{3}\right),\ 0 \le x < a \\ y_{BC}{}''(x) &= \frac{M_c}{EI} + \frac{F_c}{EI}(L-x) - \frac{S}{EI}y_{BC}(x) - \frac{q.\cos\alpha}{2EI}(L-x)^2 + \frac{1}{EI}\int_x^L (\xi - x)\,kq.\cos\alpha\,\frac{L-\xi}{b}d\xi,\ 0 \le x \le L \end{aligned} \tag{4}$$

Considering the stress distribution and restraint states along segments AB and BC of the roof beam, the boundary constraints are established as:

$$\begin{aligned} &y_{AB}(0) = 0 \qquad \theta_{AB}(0) = 0 \\ &y_{BC}(L) = 0 \qquad \theta_{BC}(L) = 0 \\ &y_{AB}(a) = y_{BC}(a) \quad \theta_{AB}(a) = \theta_{BC}(a) \end{aligned} \tag{5}$$

Based on mechanics of materials, the equations for deflection, rotation angle, and bending moment of sections AB and BC in the roof rock beam are derived as follows:

$$\begin{aligned} y_{AB}(x) &= A_1\cos\sqrt{\frac{S}{EI}}x + A_2\sin\sqrt{\frac{S}{EI}}x + \frac{kq\cos\alpha - q\cos\alpha}{2S}x^2 + \frac{qL\cos\alpha - kqa\cos\alpha - F_c}{S}x \\ &- \frac{kqb\cos\alpha}{2S} + \frac{M_c + F_cL}{S} - \frac{qL^2\cos\alpha}{2S} + \frac{kqa^2\cos\alpha}{2S} + \frac{kqb\cos\alpha}{2S}\left(a + \frac{b}{3}\right) - \frac{EI(kq\cos\alpha - q\cos\alpha)}{S^2}, \\ y_{BC}(x) &= A_3\cos\sqrt{\frac{S}{EI}}x + A_4\sin\sqrt{\frac{S}{EI}}x - \frac{kq\cos\alpha}{6bS}x^3 + \frac{kqL\cos\alpha}{2bS}x^2 - \frac{q\cos\alpha}{2S}x^2 + \frac{qL\cos\alpha - F_c}{S}x \\ &- \frac{kqL^2\cos\alpha}{2bS}x + \frac{EIkq\cos\alpha}{bS^2}x + \frac{M_c + F_cL}{S} - \frac{qL^2\cos\alpha}{2S} + \frac{L^3kq\cos\alpha}{6Sb} - \frac{LEIkq\cos\alpha}{S^2b} + \frac{EIq\cos\alpha}{S^2} \\ \theta_{AB} &= -A_1\sqrt{\frac{S}{EI}}\sin\sqrt{\frac{S}{EI}}x + A_2\sqrt{\frac{S}{EI}}\cos\sqrt{\frac{S}{EI}}x + \frac{kq\cos\alpha}{S}x - \frac{q\cos\alpha}{S}x + \frac{qL\cos\alpha - kqa\cos\alpha - F_c}{S} - \frac{kqb\cos\alpha}{2S}, \\ \theta_{BC} &= A_4\sqrt{\frac{S}{EI}}\cos\sqrt{\frac{S}{EI}}x - A_3\sqrt{\frac{S}{EI}}\sin\sqrt{\frac{S}{EI}}x - \frac{kq\cos\alpha}{2bS}x^2 + \left(\frac{kqL\cos\alpha}{bS} - \frac{q\cos\alpha}{S}\right)x + \frac{qL\cos\alpha - F_c}{S} - \frac{kqL^2\cos\alpha}{2bS} + \frac{EIkq\cos\alpha}{bS^2} \end{aligned} \tag{6}$$

(7)

$$\begin{aligned} M_{AB} &= -A_1S\cos\sqrt{\frac{S}{EI}}x - A_2S\sin\sqrt{\frac{S}{EI}}x + \frac{kq\cos\alpha - q\cos\alpha}{S}EI, \\ M_{BC} &= -A_3S\cos\sqrt{\frac{S}{EI}}x - A_4S\sin\sqrt{\frac{S}{EI}}x - \frac{EIkq\cos\alpha}{bS}x + \frac{LEIkq\cos\alpha}{Sb} - \frac{EIq\cos\alpha}{S} \end{aligned} \tag{8}$$

In the equation: A_1, A_2, A_3, A_4, F_c, and M_c are constants.

Based on the deflection, rotation angle, and bending moment equations of sections AB and BC in the roof rock beam, combined with their boundary conditions, the constants A_1, A_2, A_3, A_4, F_c, and M_c can be expressed in the following matrix form:

$$\begin{pmatrix} 1 & 0 & 0 & 0 & \frac{1}{S} & \frac{L}{S} \\ 0 & \sqrt{\frac{S}{EI}} & 0 & 0 & 0 & -\frac{1}{S} \\ 0 & 0 & \cos\sqrt{\frac{S}{EI}}L & \sin\sqrt{\frac{S}{EI}}L & \frac{1}{S} & 0 \\ 0 & 0 & -\sqrt{\frac{S}{EI}}\sin\sqrt{\frac{S}{EI}}L & \sqrt{\frac{S}{EI}}\cos\sqrt{\frac{S}{EI}}L & -\frac{1}{S} & 0 \\ -\sqrt{\frac{S}{EI}}\sin\sqrt{\frac{S}{EI}}a & \sqrt{\frac{S}{EI}}\cos\sqrt{\frac{S}{EI}}a & \sqrt{\frac{S}{EI}}\sin\sqrt{\frac{S}{EI}}a & -\sqrt{\frac{S}{EI}}\cos\sqrt{\frac{S}{EI}}a & 0 & 0 \\ \cos\sqrt{\frac{S}{EI}}a & \sin\sqrt{\frac{S}{EI}}a & -\cos\sqrt{\frac{S}{EI}}a & -\sin\sqrt{\frac{S}{EI}}a & 0 & 0 \end{pmatrix} \begin{pmatrix} A_1 \\ A_2 \\ A_3 \\ A_4 \\ M_c \\ F_c \end{pmatrix}$$

$$= \begin{pmatrix} \dfrac{q\cos\alpha\left[L^2 - ka^2 - kb\left(a + \dfrac{b}{3}\right)\right]}{2S} + \dfrac{EIq\cos\alpha\,(k-1)}{S^2} \\ \dfrac{q\cos\alpha\,[2\,(ka - L) + kb]}{2S} \\ -\dfrac{EIq\cos\alpha}{S^2} \\ -\dfrac{EIkq\cos\alpha}{bS^2} \\ \dfrac{kq\cos\alpha\left[b^2 - (L-a)^2\right]}{2bS} + \dfrac{EIkq\cos\alpha}{bS^2} \\ \dfrac{kq\cos\alpha\left[(L-a)^3 - b^3\right]}{6bS} + \dfrac{EIkq\cos\alpha\,(a+L+b)}{bS^2} \end{pmatrix} \tag{9}$$

Based on the summary of the above deflection, rotation angle, bending moment equations, and the matrix equation of the roof rock beam, it is concluded that the coal seam dip angle alters the stress state of the roof and exerts a certain influence on the deformation of the roof in steeply inclined coal seams. The length of the working face affects the deformation of the roof in steeply inclined coal seams through the exposed area of the immediate roof and the characteristics of stress distribution. The burial depth controls the initial stress state of the roof via the *in-situ* stress field, and for steeply inclined coal seams, a greater burial depth leads to more pronounced asymmetric characteristics along the inclination of the working face. Different backfill lengths significantly influence roof deformation, with full backfilling yielding the best effect. In practical engineering, partial backfilling is often adopted considering backfilling costs, making it important to determine the optimal backfill length.

2.2 Deformation and Failure Mechanisms of Roof Strata under Multifactorial Conditions

Based on the mechanical analysis of the dip-direction roof rock beam model in steeply dipping coal seams with partial backfill, together with a review of existing research, it is observed that the roof rotation angles follow a cyclical pattern of "increase–decrease–increase–decrease." The minimum values occur at both ends and the central section of the working face, whereas the peaks appear in the upper-middle and lower-middle regions. Correspondingly, roof deflection exhibits a bimodal "increase–decrease" trend, with the maximum displacement concentrated in the central zone, in contrast to the relatively lower values in the upper and lower sections. Complementing these trends, the bending moment distribution oscillates in a "decrease–increase–decrease–increase" sequence, showing higher stress levels in the upper and lower parts compared to the central area. Accordingly, using the controlled variable method, this study investigates the variation trends of roof deflection and bending moment under different influencing factors, including working face length (L), mining depth (H), coal seam dip angle (α), and backfill length (a). The aim is to clarify the response and fracture mechanisms of roof strata in steep coal seams under partial backfill conditions amid multivariable interactions.

Fig. 2 illustrates the characteristic variations in rotation angle, deflection, and bending moment of the roof beam strata under different working face lengths. Along the inclination direction, the behavior and fracture development of the roof strata exhibit pronounced spatial heterogeneity. As the unsupported roof span progressively increases, the combined influence of overburden loading and gravitational forces drives the redistribution of *in-situ* stress. This geomechanical process enhances tensile-shear composite stresses within the roof strata while simultaneously accelerating bed separation

and fracture propagation. As a result, these interacting mechanisms lead to a progressive increase in rotation angles, deflection magnitudes, and bending moment values across the roof structure.

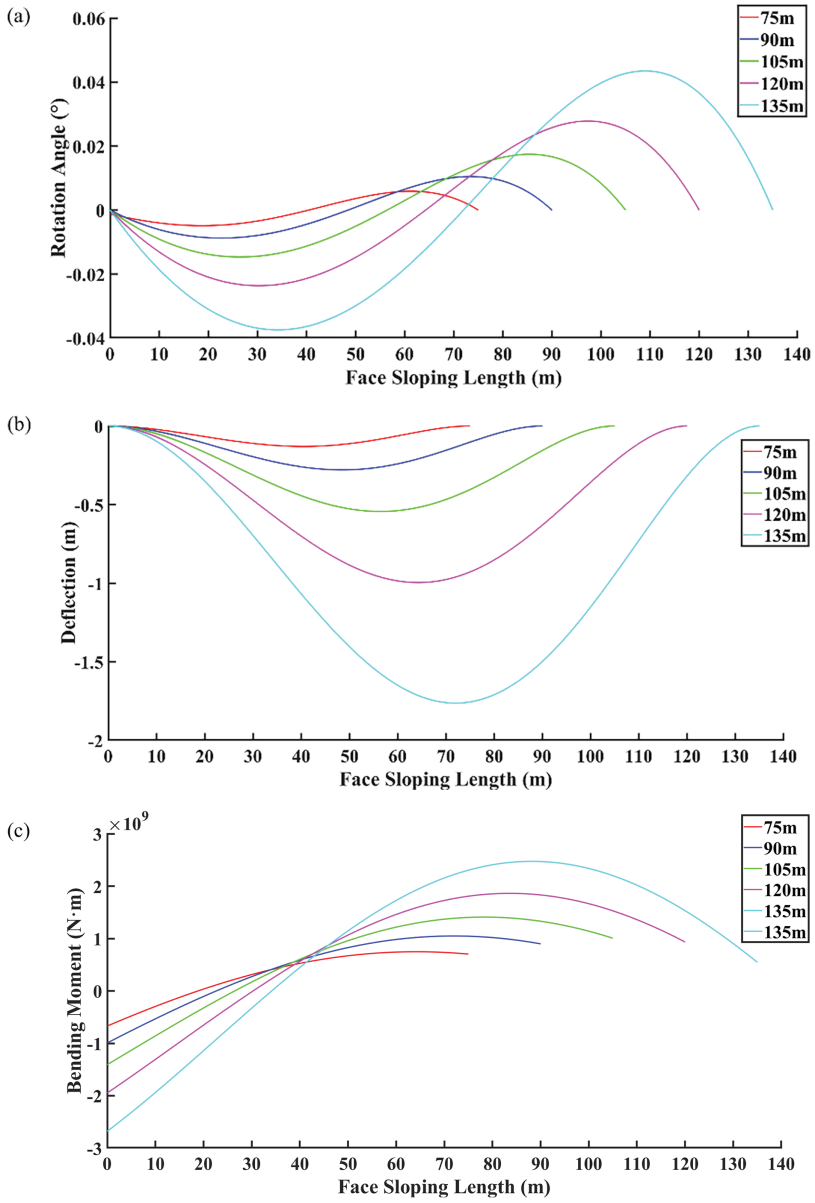

Figure 2: Variation characteristics of roof rotation angle, deflection, and bending moment under different working face lengths (a–c). (a) Rotation angle variation; (b) Deflection variation; (c) Bending moment variation

Fig. 3 depicts characteristic changes in rotation angle, deflection, and bending moment for the roof beam strata under different mining depths. As the mining depth increases, *in-situ* stresses progressively intensify. Mining-induced disturbances under high confining pressures induce more extensive bed separation and fracturing within the roof strata. Concurrently, reduced roof stiffness exacerbates flexural deformation of the rock beam, with an expanding influence zone that eventually

compromises the overall stability of overlying strata. These combined effects lead to progressive increases in rotation angle, deflection, and bending moment values.

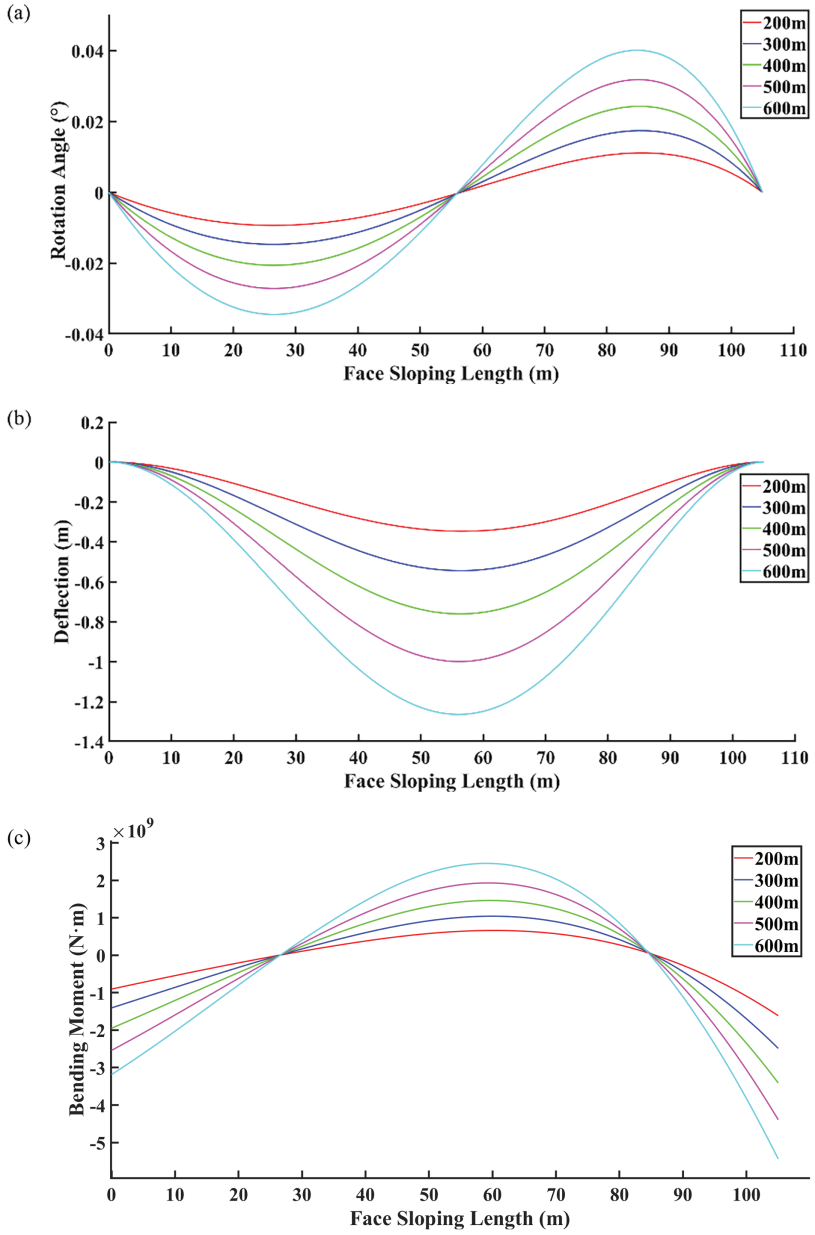

Figure 3: Variation characteristics of roof rotation angle, deflection, and bending moment under different mining depths (a–c). (a) Rotation angle variation; (b) Deflection variation; (c) Bending moment variation

Fig. 4 depicts characteristic changes in rotation angle, deflection, and bending moment for the roof beam strata under different coal seam dip angles. With increasing seam inclination, the dip-parallel gravitational influence of superincumbent strata escalates whereas the orthogonal component attenuates, resulting in reduced flexural deformation tendencies of the rock beam. Consequently, the

deflection, bending moment, and rotation angle of roof strata demonstrate systematic decreases, with progressive convergence observed between parameter values.

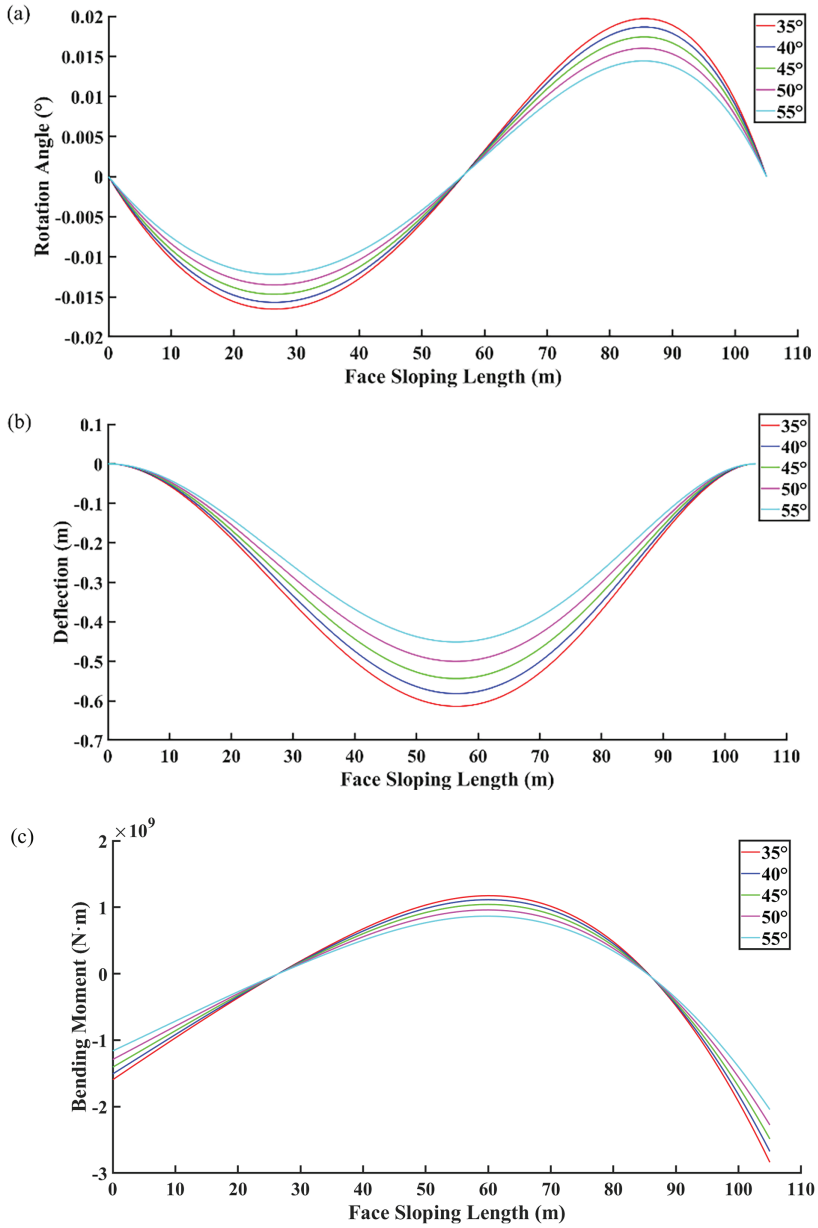

Figure 4: Variation characteristics of roof rotation angle, deflection, and bending moment under differentt coal seam dip angles (a–c). (a) Rotation angle variation; (b) Deflection variation; (c) Bending moment variation

Fig. 5 depicts characteristic changes in rotation angle, deflection, and bending moment for the roof beam strata under different backfill lengths. Increasing backfill length reduces goaf volume while enhancing the bearing capacity of backfill structures, effectively suppressing the development of roof bed separation fractures. Under steeply dipping coal seam conditions, gravitational sliding

of caved gangue toward the upper backfill zone progressively compacts the mined-out space. This mechanism significantly inhibits overlying strata subsidence, leading to systematic decreases in roof rotation angles, deflection magnitudes, and bending moment values.

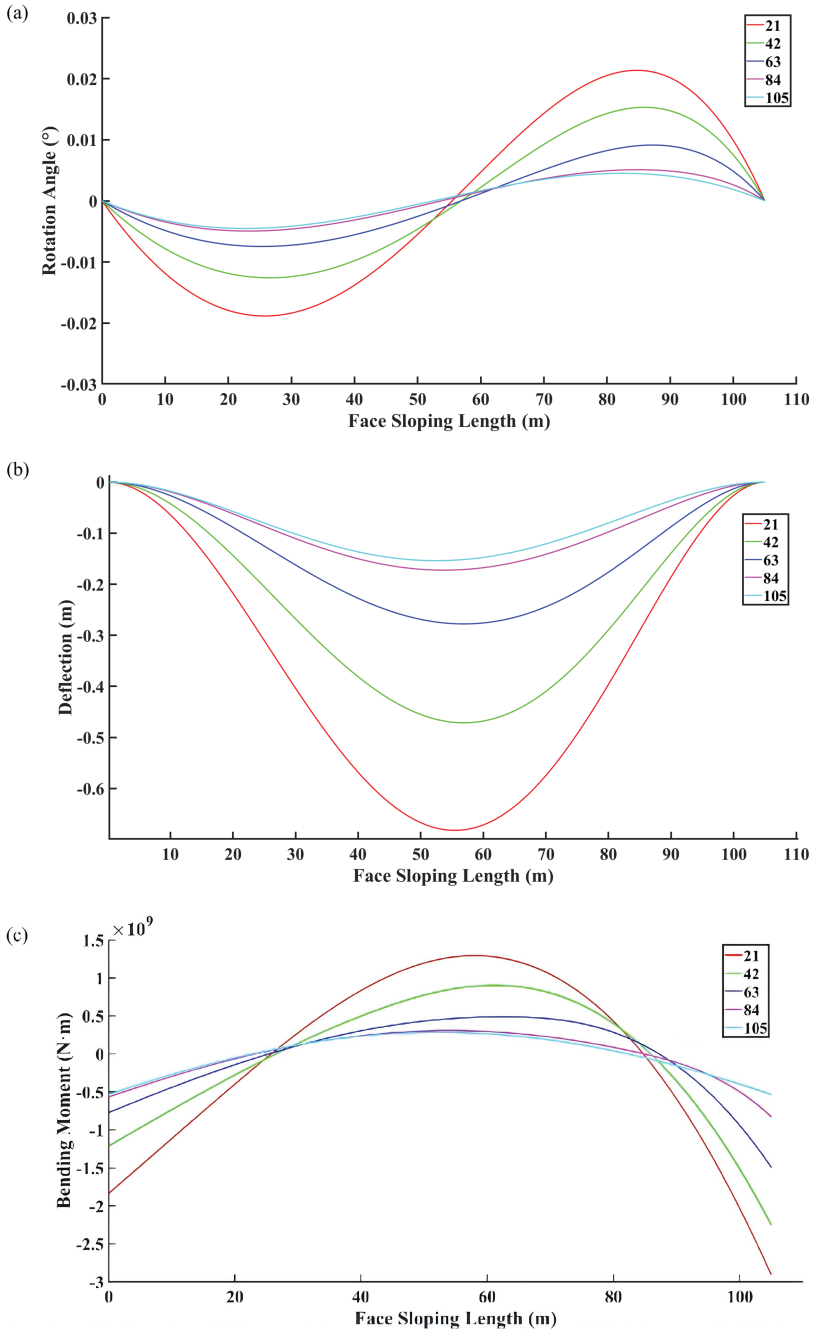

Figure 5: Variation characteristics of roof rotation angle, deflection, and bending moment under different backfill lengths. (a) Rotation angle variation; (b) Deflection variation; (c) Bending moment variation

A comparative analysis of roof deformation parameters (rotation angle, deflection, and bending moment) under different backfill lengths, combined with an economic assessment of field backfill operations, identifies backfill lengths of 21 and 63 m—corresponding to 1/5 to 3/5 of the working face length (L)—as configurations that effectively balance technical performance and economic feasibility. Within this range, the roof beam shows relatively lower deformation parameters compared with other backfill schemes while maintaining cost-effectiveness in practice. This balance between technical benefit and economic cost confirms the viability of adopting partial backfill within the 1/5–3/5 L range for improved roof stability control.

3 Deformation and Stress Characteristics of Surrounding Rock under Partial Backfill

3.1 Similar Material Simulation Experiments

The 25221-working face in a certain mine is designed with a strike length of 2098 m and an inclined length of 105 m. The coal seam dip angle ranges from 36° to 46°, with an average of 45°, and the coal density is 1.39 t/m^3. The coal seam exhibits stable geological occurrence. The stratigraphic column of the 25221 working face coal seam is shown in Fig. 6.

Comprehensive Stratigraphic Column of Coal Seam

Era	Formation	Histogram	Thickness	Stratum	Description
Jurassic	Badaowan Formation		16.59	Main Roof	Medium sandstone, grayish-white,quartz-dominated, strong weathering resistance, well-developed bedding planes
			2.32	Immediate Roof	Grayish-white pebbly coarse sandstone
			3.58-9.77 / 5.77	Coal Seam	Upper section: 2.5m coal-shale interbedded layer; Middle section: three layers of partings (0.4–0.5m thick); Base: 0.6m carbonaceous mudstone
			17.06	Immediate Floor	Blackish-gray quartz-dominated sandstone with mineral cementation
			9	Main Floor	Well-developed joints,friable when weathered

Figure 6: Composite stratigraphic column

This geologically stable coal seam's stratigraphic sequence is detailed in Fig. 6.

Based on the physico-mechanical parameters of rock strata in the 25221 working face and the dimensions of the experimental frame, a three-dimensional similarity simulation apparatus of 1500 mm × 600 mm × 1500 mm was utilized. The similarity constants were determined as a geometric similarity ratio of 1:100, a density similarity constant of 1.6, a stress similarity constant of 160, and a model dip angle of 45°. River sand was selected as the aggregate with gypsum and lime powder as binding materials. The material proportions were designed based on geological data of the simulated strata, mechanical properties of overlying rocks, and similarity theory, with partial similarity material ratios provided in Table 1.

Table 1: Similar material ratios for the model

No.	Lithology	Model Thickness (m)	Stratum Thickness (m)	Material Ratio	Number of Layers
1	Grey-white coarse sandstone	0.09	0.9	828	1
2	Carbonaceous mudstone	0.17	1.7	828	3
3	Coal Seam	0.05	5	20:1:3:15	1
4	Grey-white conglomerate sandstone	0.21	2.1	846	10
5	Grey-white medium sandstone	0.26	2.6	746	10

As established in previous section, partial gob backfills lengths within one-third to one-half of the working face length demonstrate optimal control over roof stability. Building on this foundation, 3D geomechanical simulations were performed under partial gob backfill conditions at the 2/5 position of the steeply dipping coal seam to investigate failure-induced displacement and stress evolution characteristics in overlying strata. The experimental setup and apparatus are illustrated in Fig. 7.

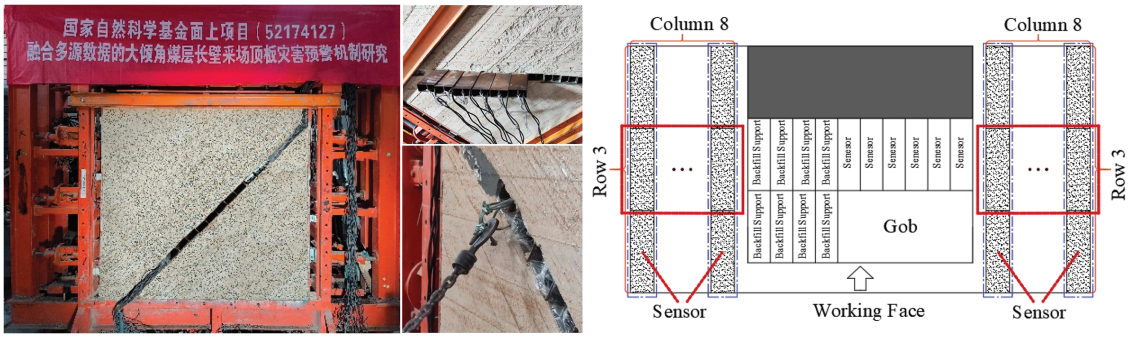

Figure 7: The experimental setup and apparatus

3.2 Movement and Evolution Characteristics of Overlying Strata in the Working Face

After coal seam extraction, mining-induced stresses initiate distress response and fracture development in the rock mass, leading to its displacement into the excavated space. Overburden failure patterns vs. advancing face distances are depicted in Fig. 8.

Following partial waste rock backfilling in steeply dipping coal seams, significant stress redistribution occurs within the surrounding rock mass of unfilled zones. Mining-induced stress redistribution triggers fracture propagation in the overburden directly above the longwall face, exhibiting distinct kinematic behaviors: the lower strata slide downward along the dip direction, while the middle-upper strata undergo asymmetric migration. Together, they progressively form an arched voussoir structure through gradual accumulation. As the face advances, large-scale roof suspension develops in unfilled

zones. At an advancement of 15 cm, the suspended roof area expands noticeably. Under the combined effect of mining-induced stress and gravitational loading, roof collapse initiates in the upper unfilled zones. The collapsed debris accumulates at the interface between the backfill and unfilled areas, establishing a roof-contact zone. Simultaneously, bed separation fractures begin to develop within the main roof due to overburden gravitational loading. Upon reaching 20 cm of advancement, sequential collapse of the immediate roof strata takes place. The resulting caved overburden self-organizes into an interlocking voussoir configuration along the dip direction, whereas deeper sections along the strike direction display disordered arrangements of rock blocks with reduced fragmentation sizes. When the advancement reaches the 40 cm threshold, the main roof in the unfilled zones experiences primary collapse, accompanied by dip-directional gravitational sliding that intensifies the failure of the overburden. Quantitative measurements record the following: a residual step length of 2.1 cm at upper-end roof fractures, a strike-parallel extension of 9 cm in fractured roof remnants, and a dip-length persistence of 4 cm in lower immediate roof sections.

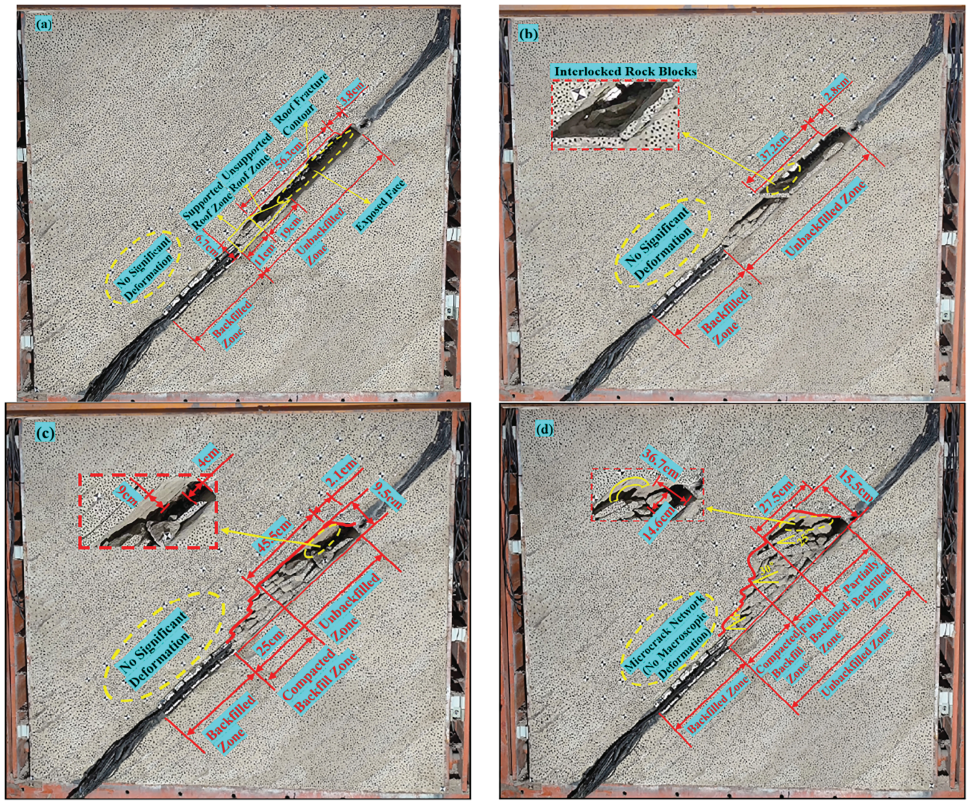

Figure 8: Overburden failure patterns vs. advancing face distances (a–d). (a) Working face advancement at 15 cm; (b) Working face advancement at 20 cm; (c) Working face advancement at 40 cm; (d) Working face advancement at 60 cm

Within the backfilled zones, the backfill structure bears both the overburden load and the stress transferred from intact key strata in adjacent unbackilled regions. Due to gravitational displacement, partially collapsed gangue from unbackfilled areas undergoes progressive sliding and accumulation on top of the backfill material, resulting in a non-uniform packing configuration. By the time the face advances 40 cm, dip-oriented fracture networks become more pronounced within the roof strata of

the backfilled zone. These fractures develop through a dual mechanism: stress relaxation following initial main roof failure in neighboring unbackfilled zones, combined with stress concentration in the upper part of the backfilled area induced by mining-related stress redistribution. Simultaneously, roof collapse in unbackfilled zones leads to the accumulation of debris at the base while creating voids above, which facilitate further strata deformation and stress evolution. When the face advances to 60 cm, more extensive failure of the main roof in unbackfilled zones promotes broader gangue backfilling across the mid-lower dip sections. Based on backfill density, the goaf can be vertically divided into three distinct zones: an upper compacted zone (inclined at 35°), an intermediate fully packed zone (30°), and a lower partially filled zone (25°)—each defined by a characteristic angle of gangue stacking relative to the horizontal.

Digital Image Correlation (DIC) is a modern optical measurement method based on speckle image analysis, also referred to as digital speckle metrology. In the experiment, DIC directly provides full-field deformation results with high spatial resolution. The evolution patterns of horizontal, vertical, and resultant displacements of surrounding rock under different advancement distances are shown in Figs. 9–12.

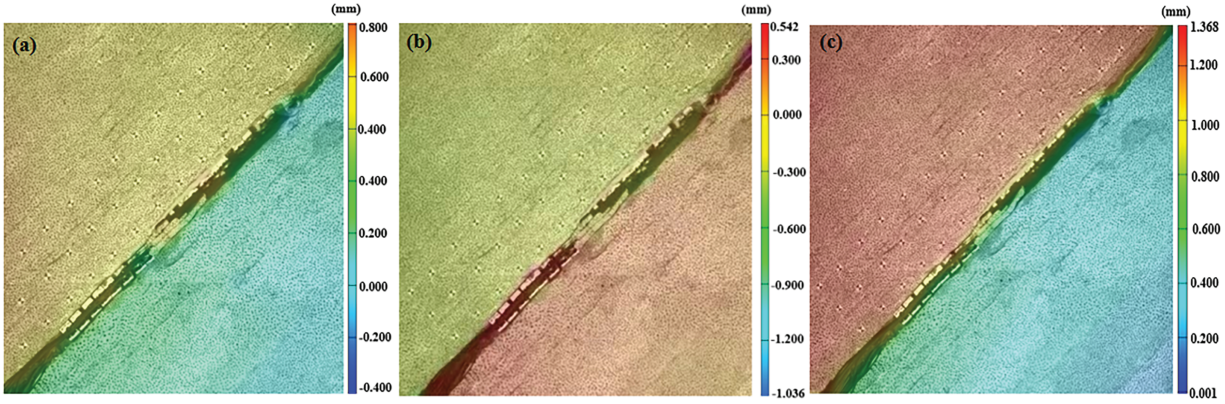

Figure 9: Surrounding rock displacement at 15 cm advance (a–c). (a) Horizontal displacements; (b) Vertical displacements; (c) Resultant displacements

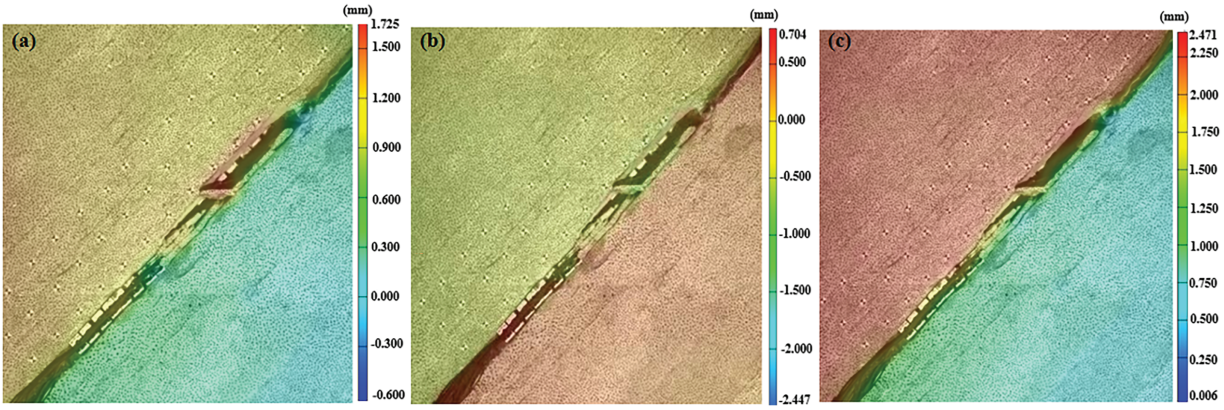

Figure 10: Surrounding rock displacement at 20 cm advance (a–c). (a) Horizontal displacements; (b) Vertical displacements; (c) Resultant displacements

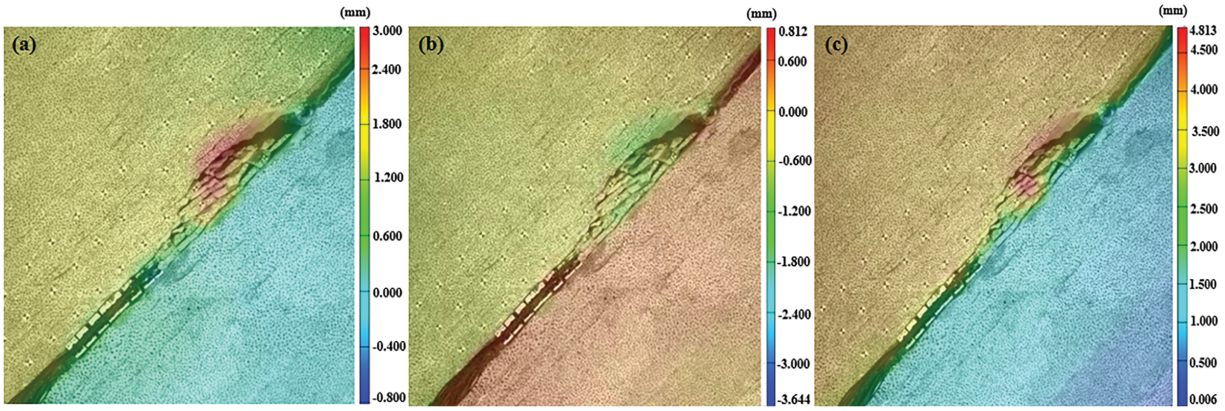

Figure 11: Surrounding rock displacement at 40 cm advance (a–c). (a) Horizontal displacements; (b) Vertical displacements; (c) Resultant displacements

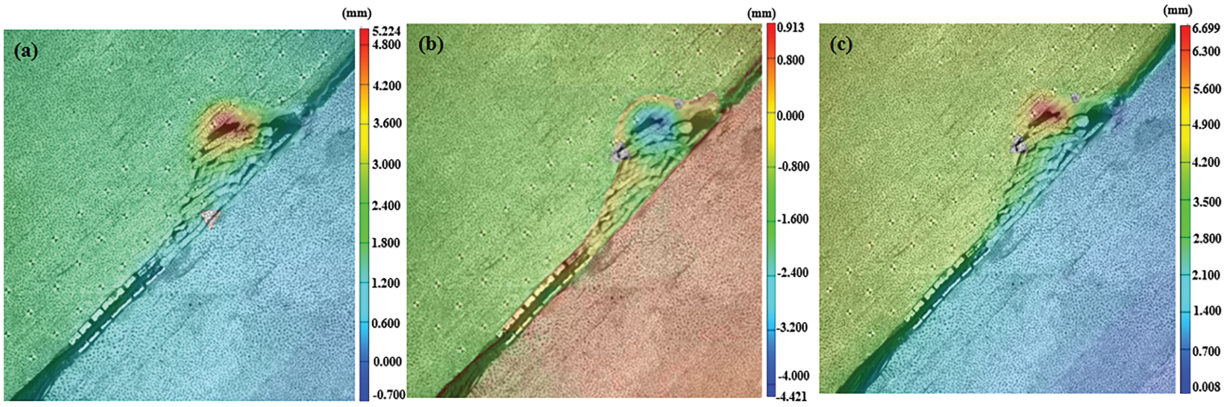

Figure 12: Surrounding rock displacement at 60 cm advance (a–c). (a) Horizontal displacements; (b) Vertical displacements; (c) Resultant displacements

The analytical results demonstrate distinct displacement characteristics at different advancement stages: horizontal displacement increased by 115.6%, 73.9%, and 74.1% at 15, 20, and 40 cm, respectively, while vertical displacement rose 136.2%, 48.9%, and 21.3%. Resultant displacement exhibited growth rates of 80.6%, 94.8%, and 39.2%, correspondingly. Throughout continuous extraction, surrounding rock deformation followed consistent "stabilization-growth-restabilization" sequences across all displacement vectors. This evolutionary pattern initiated with minor roof fracturing during initial mining phases, progressively intensifying with face advancement. Displacement propagation originated from upper-central sections of the unfilled zone along the dip direction, subsequently diffusing toward central and mid-lower regions.

With the progression of the working face in the strike direction, the fracture elevation of roof strata within the unbackfilled zone progressively rises from the lower to upper sections along the dip. Simultaneously, the apex of the arched shell structure gradually elevates, resulting in decreased structural integrity of the upper rock layers. Furthermore, during the upward evolution of the arched shell vertex (arch crown) toward higher-level strata, the upper arch abutment migrates toward the upper-end coal pillar zone, while the lower arch abutment extends into the backfilled zone. This

confirms that partial gob backfill effectively regulates the evolutionary behavior of overburden during extraction within steep coal seams.

3.3 Analysis of Stress Patterns in Backfill Body of Backfilled Zone

To investigate strata pressure behavior patterns in steeply dipping coal seams with partial gangue backfill, wired pressure sensors were strategically deployed to acquire pressure measurements at key monitoring stations. The collected datasets underwent systematic processing and interpretation, establishing a theoretical framework for analyzing ground pressure manifestation mechanisms in longwall mining operations.

To characterize ground pressure behavior in steeply dipping coal seams with partial waste rock backfilling, wired pressure transducers were strategically deployed across dip-directional monitoring stations (upper, central, and lower sections) within backfilled zones. The acquired pressure data underwent systematic processing to establish theoretical foundations for analyzing working face pressure distribution patterns, with recorded pressure measurements systematically presented in Fig. 13.

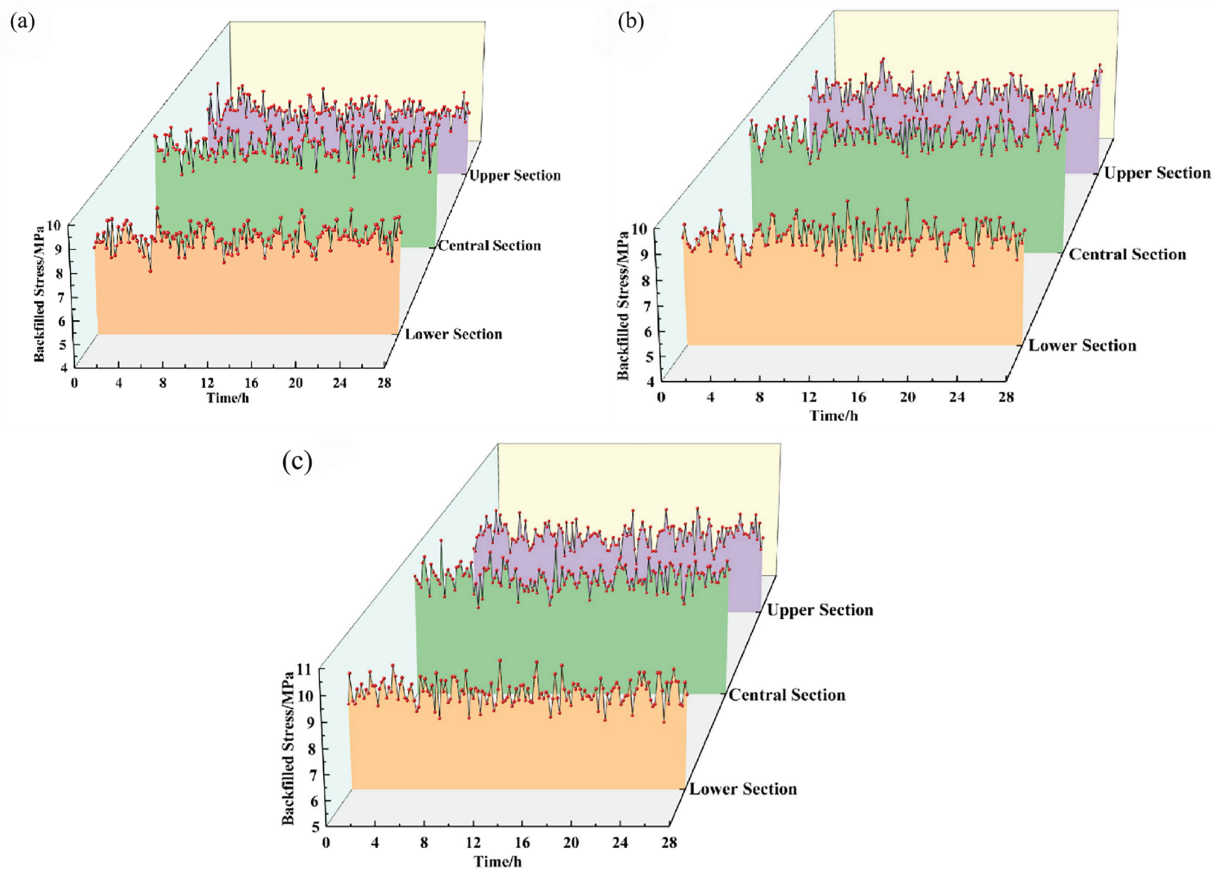

Figure 13: Stress patterns of backfill body in backfilled zone of working face. (a) Working face advancement at 20 cm; (b) Working face advancement at 40 cm; (c) Working face advancement at 60 cm

Monitoring results indicate that at advancement distances of 20, 40, and 60 cm, the mean stress magnitudes in the backfill's upper dip region reach 8.65, 7.79, and 8.45 MPa, respectively; in the central section, the values are 9.86, 9.15, and 9.86 MPa; and in the lower section, the values are 8.82, 8.41, and 8.83 MPa. Analytical results demonstrate that the backfill body exhibits a stress concentration tendency in its central zone along the working face's dip orientation, moderate stress in the lower section, and minimum stress in the upper section. This phenomenon arises because the backfill body bears the overburden loads transmitted from the unbroken key strata, thereby influencing the stress redistribution in the stope. The central section of the backfill body, acting as the core load-bearing zone, experiences a superimposed effect of dip-direction stress and upper-section transmitted stress, resulting in a stress concentration area characterized by elevated stress levels. The upper backfill section neighboring the goaf develops a stress-relaxed zone, with overburden pressure shifting to the interior backfilled areas and consequently inducing stress reduction in this zone. The lower section of the backfill body, located at the lowermost part of the backfilled zone, lies at the end of the load transfer path, where the influence of overburden load transfer relatively diminishes. Additionally, this section bears partial gravitational load of the backfill body, leading to higher stress than the upper section but lower than the central section.

3.4 Analysis of Support Resistance Patterns in Unbackfilled Zone

This investigation primarily examines the support resistance characteristics in the unfilled regions of longwall mining faces. Simplified supports (with wired pressure sensors) installed at different elevations of the unfilled zone—including lower, intermediate, upper-intermediate and top regions—were chosen for analysis. Specifically, the shield resistance data of supports #26, #30, #33, and #36 along the coal seam mining direction are shown in Fig. 14.

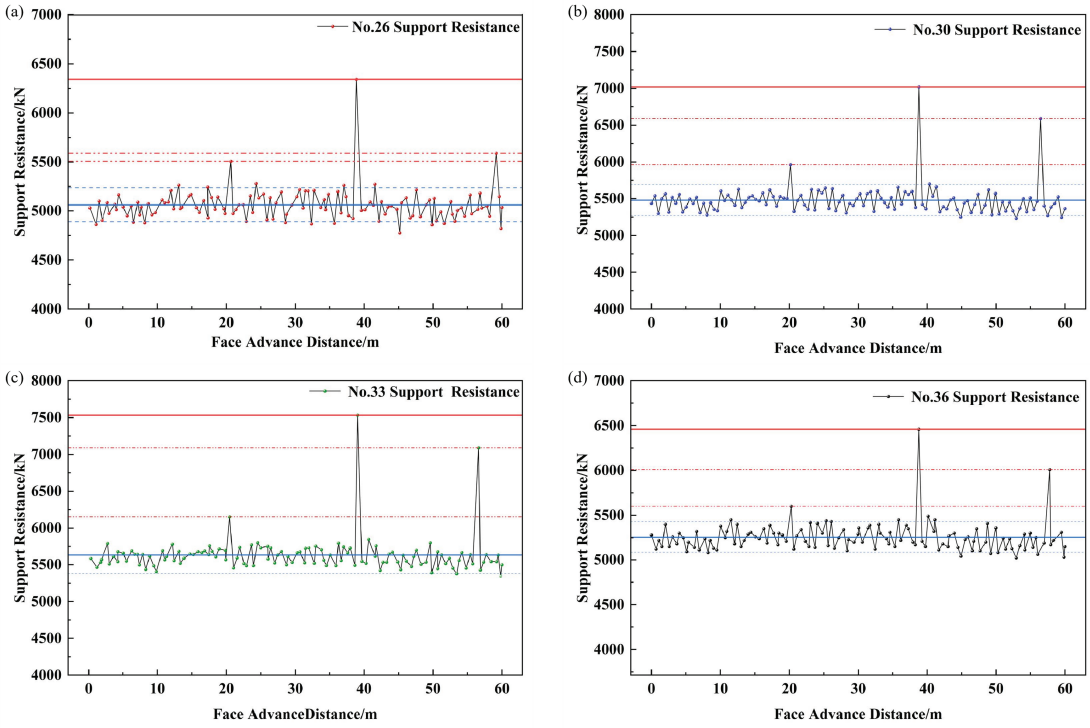

Figure 14: Support working resistance distribution in coal seam mining. (a) No. 26 support resistance; (b) No. 30 support resistance; (c) No. 33 support resistance; (d) No. 36 support resistance

Fig. 14 illustrates the continuous variation of shield loads with face advance during experimentation. The shield resistance, weighting interval, and weighting intensity exhibited marked regional differences across the working face, with average working resistances measuring 6301 (lower section), 7019 (middle), 7531 (upper-middle), and 6459 kN (upper), corresponding to specific roof strata movement patterns.

At 20.2 cm of face advance, initial caving of the immediate roof in the unfilled zone induced stress redistribution, prompting differential increases in shield resistance throughout the face. Subsequent main roof fracturing at 39.1 cm advancement caused abrupt resistance escalation, particularly at the upper-middle #33 support (14.1% peak increase). This mechanical response originated from the backfill' s partial load-bearing in the lower unfilled zone, while the upper-middle roof sustained maximum pressure (7531 kN) through combined self-weight and overburden loading.

The 56–59 cm advancement phase witnessed simultaneous first periodic weighting at supports #26, #30, #33, and #36, recording average resistances of 5589, 6589, 7089, and 6009 kN, respectively. Weighting intervals of 20, 17.4, 17.5, and 18.9 cm established a clear temporal sequence: upper-middle → middle → lower → upper sections, confirming measurable hysteresis in peripheral regions.

As shown in Fig. 15, the bar charts and their corresponding fitting curves collectively illustrate the working resistance (kN) of hydraulic supports at different positions (lower, middle, upper-middle, and upper sections) under various mining conditions. The analysis reveals that the upper-middle and middle sections constitute distinct stress concentration zones, whereas the lower and upper sections function as stress relief zones.

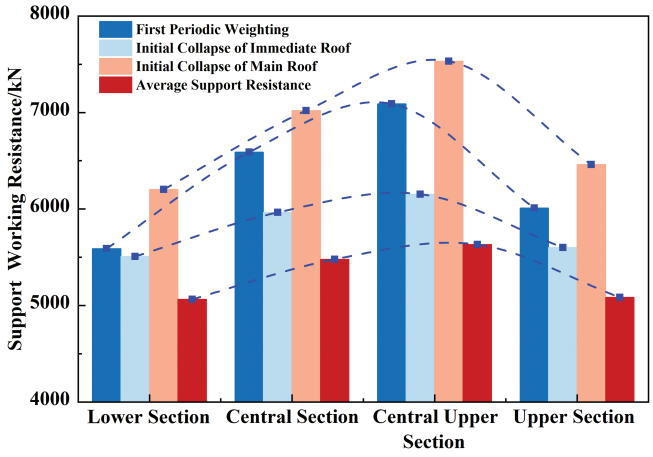

Figure 15: Histogram of support resistance at different positions in unbackfilled zone

In unfilled areas, the working resistance values of supports consistently followed a characteristic descending order: upper-middle section > middle section > upper section > lower section. Strata within the lower unfilled zone exhibited substantially reduced activity levels, contrasting sharply with heightened activity documented in the mid-upper and upper mining zones. With progressive face advancement, the expanding contact area between backfilled gangue and roof strata led to a pronounced reduction in ground pressure manifestations across different zones, accompanied by steadily improving stability of the overlying strata structures. These results substantiate that partial gangue backfilling serves as an effective measure for controlling roof pressure in steeply dipping coal seams.

The physical similarity simulation experiment provides robust experimental validation for the core conclusions derived from the theoretical analysis in Section 2. Specifically, it confirms that implementing partial backfill within the range of one-third to one-half of the working face length at the lower section effectively controls roof stability and reveals the inherent characteristics of asymmetric deformation and failure in the overburden under steeply inclined conditions. Subsequently, an in-depth analysis will be conducted by establishing a FLAC3D numerical model to examine the overburden movement patterns, strata behavior characteristics, and plastic failure mechanisms under partial backfill mining.

4 Numerical Simulation Study on Partial Gob Backfill Mining

4.1 Model Design

(1) Computing software

FLAC3D, developed by Itasca Consulting Group (USA), is a three-dimensional explicit finite-difference software widely recognized in the coal mining industry for its robust computational capabilities and versatile simulation functions. It efficiently simulates complex mining scenarios through parameter input, rational boundary conditions, and optimized mesh generation, while intuitively presenting results—such as stress distribution, displacement fields, and plastic zone evolution—via contour plots, thereby supporting effective mine monitoring. Its computational accuracy has been extensively validated, making it a reliable tool for verifying physical similarity experiments and simulating real-world mining conditions. Importantly, FLAC3D is particularly suited for this study due to its core strength in simulating large deformations, plastic failure, and stress redistribution in geomaterials. The software's material models and computational architecture are adept at handling the discontinuous and nonlinear mechanical behavior of surrounding rock under complex mining conditions. Given that this research focuses on overburden movement, stress-arch evolution, and plastic zone extension induced by partial backfill mining in steeply dipping coal seams—processes involving significant material yielding and failure—FLAC3D provides an accurate and methodologically appropriate platform for characterizing strata response under such specific geological and mining settings.

(2) Calculation parameters

Conduct experiments based on the stratigraphic information and geological data of the 25221-working face. The physical and mechanical parameters obtained are shown in Table 2.

Table 2: Mechanical parameters of coal and rock strata

No.	Rock Name	Bulk Density (kg/m^3)	Elastic Modulus (MPa)	Poisson's Ratio	Compressive Strength (MPa)	Cohesion (MPa)	Internal Friction Angle (°)
1	Gray-white fine sandstone	2550	0.82×10^4	0.15	3.5	5.2	35
2	Gray-white medium sandstone	2675	0.12×10^4	0.31	2.9	1.0	25

(Continued)

Table 2 (continued)

No.	Rock Name	Bulk Density (kg/m^3)	Elastic Modulus (MPa)	Poisson's Ratio	Compressive Strength (MPa)	Cohesion (MPa)	Internal Friction Angle (°)
3	Gray-white gravelly coarse sandstone	2662	0.2×10^4	0.26	1.1	0.8	23
4	Siltstone	2710	1.4×10^4	0.24	2.0	1.8	31
5	Carbonaceous mudstone	1500	0.2×10^4	0.35	1.1	0.8	23
6	No. 5 Coal Seam	1350	0.3×10^4	0.30	0.4	1.6	28
7	Gangue backfill	1200	0.5×10^4	0.24	0	0.8	21
8	Carbonaceous mudstone	1500	0.2×10^4	0.35	1.1	0.8	23
9	Gray-white coarse sandstone	2492	2.0×10^4	0.21	1.8	3.1	35
10	Gray-black siltstone	2710	1.4×10^4	0.24	2.0	1.8	31

(3) Computational model

Based on the three-dimensional physical similarity simulation experiment, the numerical simulation mechanical model was established as shown in Fig. 16. To mitigate boundary constraint effects during computation, horizontal displacement constraints were applied to the front, rear, left, and right lateral surfaces, while vertical displacement constraints were imposed at the model base. To enhance simulation realism, a mining space was created beyond the boundary-affected zone. A uniformly distributed vertical load was applied to the model's top boundary according to *in-situ* rock stress conditions. The magnitude of this load was determined by:

$$q = \gamma H \tag{10}$$

where:

γ = unit weight of overburden rock (25 kN/m^3)

H = distance from model top boundary to ground surface (m).

Given the actual overburden thickness of 200 m, an equivalent load of 5.0 MPa was applied to the model top boundary.

(4) Numerical model

Using FLAC3D, a 3D numerical model was developed based on the mechanical framework to investigate partial gangue backfill mining in the coal seam. The numerical model was configured with a geometric domain of 150 m (X) × 80 m (Y) × 150 m (Z), with a working face length of 105 m and a specified seam thickness h = 5 m. The Mohr-Coulomb constitutive model was employed to simulate the irreversible plastic deformation of surrounding rocks after coal seam extraction. The model comprised 501,120 elements and 519,049 nodes. The face advanced along the positive Y-axis direction for 80 m, adopting the same downward mining method as in the physical similarity experiment, as illustrated in Fig. 17.

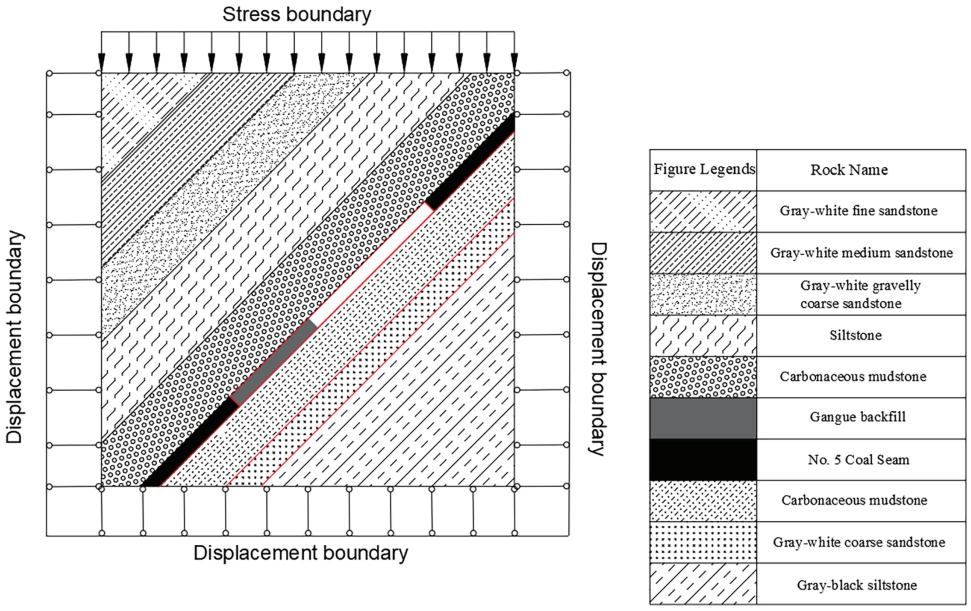

Figure 16: Numerical simulation mechanical model

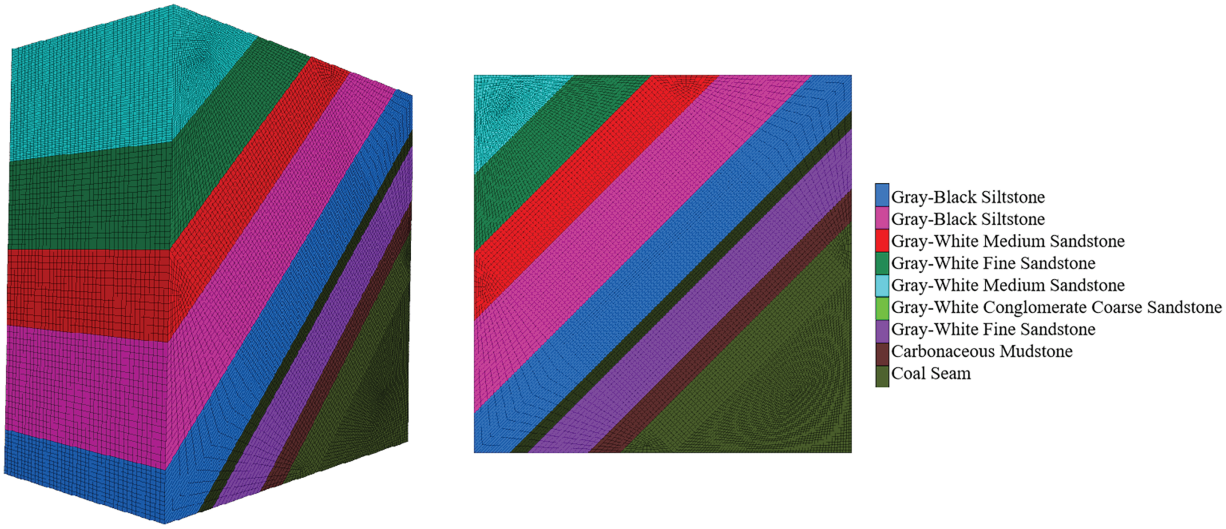

Figure 17: 3D numerical simulation model

To deepen the understanding of roof stability under partial backfilling conditions, this chapter aligns with the theoretical analysis by employing numerical simulations that systematically vary working face lengths (90, 105, 120 m) and backfill lengths (21, 42, 63 m). This multi-parametric approach enables a comprehensive investigation into the movement characteristics of overlying strata and the associated strata behavior under different controlling factors. Through this methodology, the study aims to elucidate the underlying mechanism for optimal parameter selection during coal seam extraction under multi-factor conditions.

(5) Backfill body simulation in numerical model

To ensure data integrity and model accuracy, the partial backfilling process in the FLAC3D numerical simulation is implemented as follows: First, the "excavate" command is applied to initiate face excavation, and the post-excavation model state is saved. Next, new material properties are assigned to the designated backfill zone. The "fill" command is then executed to restore and backfill the excavated area. Finally, the model equilibrium is recalculated after backfilling, and the stabilized state is saved.

By maintaining a constant working face length (consistent with the physical similarity simulation experiment) and varying the backfill ratios to 1/5, 2/5, and 3/5, this study investigates the overlying strata movement and strata pressure behavior under different backfill conditions. The optimal backfill ratio is identified through comparative analysis of the results.

4.2 Analysis of Results under Identical Working Face Length and Different Backfill Ratios

(1) Stress Distribution Characteristics of Overlying Strata

Under constant working face length conditions, partial backfilling was implemented in the steeply inclined coal seam at ratios of 1/5, 2/5, and 3/5 from the bottom upward, with the corresponding stress nephograms shown in Fig. 18, the color gradient from red to blue in the figure not only represents the magnitude variation of stress but also indicates its direction, where red denotes the positive direction and blue signifies the negative direction, with units in Pa. The results demonstrate that as the backfill ratio gradually increases, the pressure relief condition in the overlying strata of the working face progressively weakens, the scope of the stress field gradually reduces, and the stress concentration phenomenon on both the top and bottom coal pillars also gradually diminishes. This behavior is fundamentally governed by the distinct asymmetric profile of the stress arch within the overlying strata of steeply inclined coal seams. With increasing backfill ratio, this asymmetric structure is progressively optimized, enabling more effective load transfer. During the continuous backfilling process at the working face base, the backfill body acts as a critical supporting medium, not only carrying part of the overburden but also actively redistributing stresses that would otherwise concentrate around the goaf. By altering the original stress transmission path, the backfill progressively bears a greater share of the overlying load, thereby mitigating stress concentration in surrounding coal pillars.

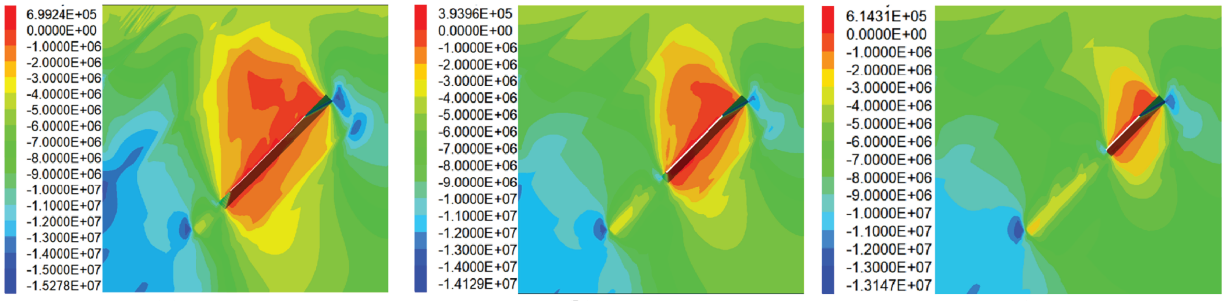

Figure 18: Vertical stress nephograms of overlying strata in steeply inclined coal seams under different backfill ratios. (a) Working face with 1/5 backfilling; (b) Working face with 2/5 backfilling; (c) Working face with 3/5 backfilling

The Fig. 19 illustrates the vertical stress monitoring profiles at the working face roof under progressively increased backfill ratios of 1/5, 2/5, and 3/5 in the steeply inclined coal seam. Analysis

indicates that stress concentration occurs at the lower end of the working face during operations, with the maximum stress values measured at 15.65, 14.45, and 13.80 MPa under progressively increased backfill ratios, showing successive reductions of 7.67% and 4.50%, respectively. Furthermore, two distinct stress relief zones are observed along the inclination direction of the working face, with the extent of these stress-relieved areas expanding as the backfill ratio increases. This pattern confirms the enhanced load-bearing capacity provided by the backfill material, which strengthens progressively with higher backfill ratios.

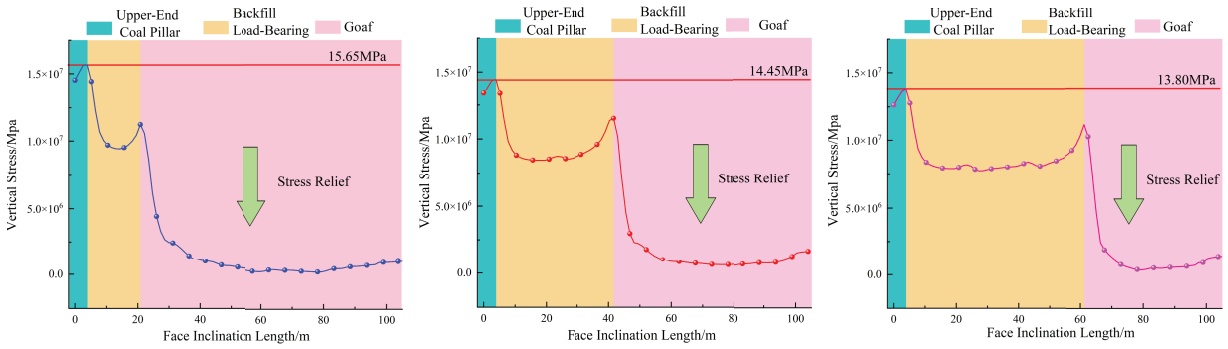

Figure 19: Vertical stress profiles of roof in steeply inclined coal seams under different backfill ratios. (a) Working face with 1/5 backfilling; (b) Working face with 2/5 backfilling; (c) Working face with 3/5 backfilling

(2) Displacement Distribution Characteristics of Overlying Strata

Under constant working face length conditions, partial backfilling was applied to the steeply inclined coal seam at ratios of 1/5, 2/5, and 3/5 from the bottom upward, with the corresponding displacement nephograms shown in Fig. 20, the color gradient from red to blue in the figure not only represents the magnitude variation of displacement but also indicates its direction, where red denotes the positive direction (upward displacement) and blue signifies the negative direction (downward displacement), with units in meters (m). The results indicate that during partial backfilling of the working face, the maximum roof subsidence displacement in the goaf decreases significantly, the displacement gradient within the overlying strata tends to moderate, and strata movement in the middle and lower sections of the goaf is effectively suppressed. Analysis reveals that the displacement field of the overlying strata in the goaf exhibits the largest influence range at a backfill ratio of 1/5, where the displacement field even locally extends to the surface, indicating that this backfill ratio fails to meet the control requirements for overlying strata and surface movement. At a backfill ratio of 2/5, a substantial reduction in the range of the displacement field is observed, with the variation bands becoming more diverse and concentrated, suggesting a gradual and progressive displacement transition between the overlying strata layers, which reflects a relatively stable condition. When the backfill ratio increases from 2/5 to 3/5, the displacement field of the overlying strata in the goaf is further reduced, but the extent of this reduction is significantly limited.

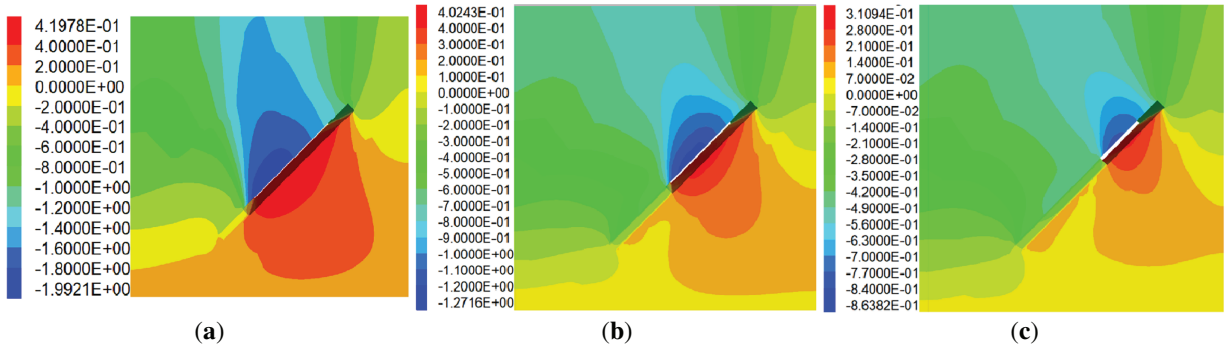

Figure 20: Vertical displacement nephograms of overlying strata in steeply inclined coal seams under different backfill ratios. (a) Working face with 1/5 backfilling; (b) Working face with 2/5 backfilling; (c) Working face with 3/5 backfilling

Fig. 21 presents the displacement monitoring curves at the roof of the working face mid-length under 1/5, 2/5, and 3/5 backfilling conditions from the bottom upward in the steeply inclined coal seam. The results show that as the backfill ratio progressively increases, the maximum roof displacements in the goaf measure 1.78, 1.08, and 0.74 m, with reduction rates of 39.3% and 31.5%, respectively. Furthermore, the inflection points on the displacement curves consistently shift toward the right side of the coordinates with increasing backfill ratios. This demonstrates that the backfill body provides enhanced support resistance as its proportion increases, effectively constraining the deformation development of the roof strata. The notable rightward shift of the inflection points indicates a significant delay in the main roof rupture and a substantial improvement in the overall stability of the roof structure, confirming the adequate backfilling in controlling strata movement.

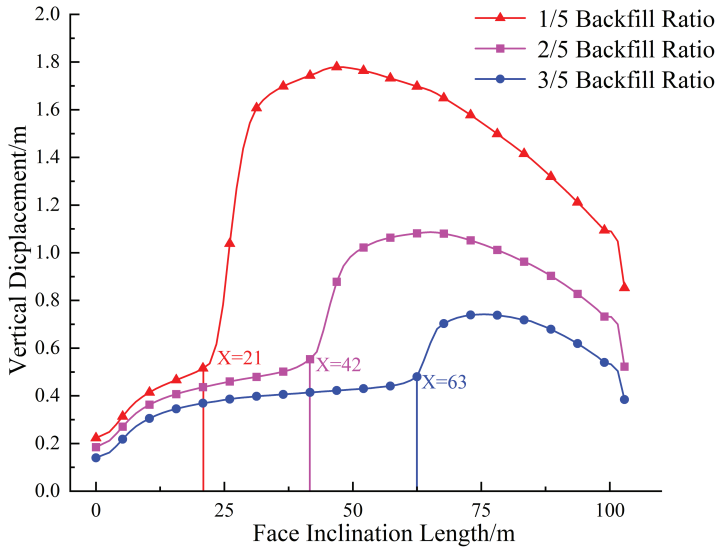

Figure 21: Vertical displacement profiles of roof in steeply inclined coal seams under different backfill ratios

(3) Plastic Failure Characteristics of Overlying Strata

Under constant working face length conditions, partial backfilling was implemented in the steeply inclined coal seam at ratios of 1/5, 2/5, and 3/5 from the bottom upward, with the corresponding plastic zone nephograms presented in Fig. 22. Analysis indicates that during the backfill mining process, the development of the plastic zone in the overlying strata of the goaf gradually weakens as the backfill ratio increases. The most significant reduction in both the height and expansion of the plastic zone occurs when the backfill ratio increases from 1/5 to 2/5. Furthermore, beyond a backfill ratio of 2/5, the development pattern of the plastic zone in the overlying strata and backfill body stabilizes, exhibiting an overall asymmetric arch structure. This demonstrates that at a backfill ratio of 2/5, the plastic failure of the overlying strata has reached a controlled and idealized state.

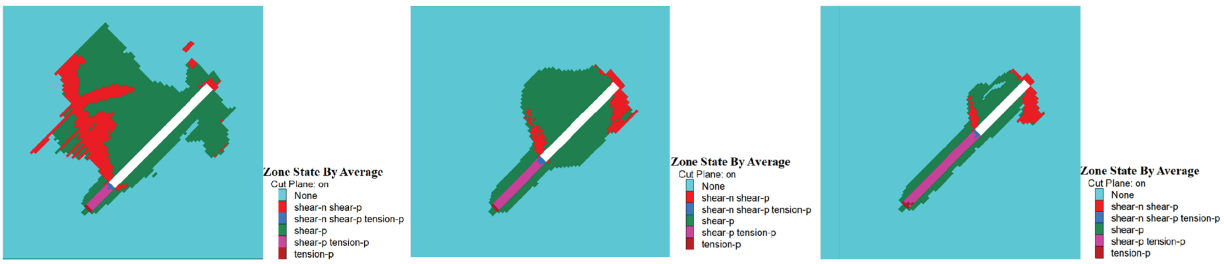

(**a**) (**b**) (**c**)

Figure 22: Failure characteristics of overlying strata in steeply inclined coal seams under different backfill ratios. (a) Working face with 1/5 backfilling; (b) Working face with 2/5 backfilling; (c) Working face with 3/5 backfilling

Based on comprehensive analysis across multiple parameters, the 2/5 backfill ratio proves to be the optimal solution for controlling the stability of steeply inclined coal seams. Stress analysis demonstrates that this ratio effectively reduces stress concentration at the working face ends while maintaining appropriate pressure relief in the overlying strata. Displacement evaluation confirms that the 2/5 ratio establishes a stable load-bearing structure, significantly reducing roof displacement with characteristic improvements in deformation patterns. Plastic zone development further validates that this ratio represents a critical threshold where rock failure becomes effectively controlled through the formation of a stable asymmetric arch structure. Although increasing the backfill ratio to 3/5 provides additional improvements, the marginal gains in stress reduction and displacement control do not justify the increased material investment. Therefore, based on the comprehensive numerical simulation results, the 2/5 backfill ratio demonstrates optimal performance in balancing control effectiveness and economic efficiency, establishing it as the most favorable backfill proportion under the given conditions.

Following the determination of the 2/5 backfill ratio as optimal, this study proceeds to investigate the most suitable inclination length for the steeply inclined coal seam working face. Integrated with theoretical analysis and physical similarity simulation experiments, the research examines overlying strata movement and strata behavior under working face lengths of 90, 105, and 120 m at the established 2/5 backfill ratio. The study further explores failure characteristics of the overlying strata across different working face lengths, with the optimal dimension to be determined through comparative analysis of the results.

4.3 Analysis of Results under Identical Backfill Ratios and Different Working Face Length

(1) Stress Distribution Characteristics of Overlying Strata

Under a constant backfill ratio of 2/5, vertical stress nephograms were obtained under different working face inclination lengths, as shown in Fig. 23, the color gradient from red to blue in the figure not only represents the magnitude variation of stress but also indicates its direction, where red denotes the positive direction and blue signifies the negative direction, with units in Pa. Analysis indicates that as the working face length increases, the extent of stress concentration zones at both ends of the working face gradually expands. At a working face length of 120 m, the upper-end coal pillar experiences peak stress concentration with a sharp increase in scope, while multiple stress concentration zones emerge at the lower-end coal pillar. When the working face length decreases to 90 m, the pressure relief extent in the goaf roof is noticeably constrained, with relatively underdeveloped stress arch structure in the roof, while significant stress concentration zones persist at both ends. In contrast, under the 105 m working face length condition, the stress concentration zones exhibit moderate expansion without abrupt local intensification, accompanied by significantly improved pressure relief extent in the roof and the formation of a relatively complete stress arch structure.

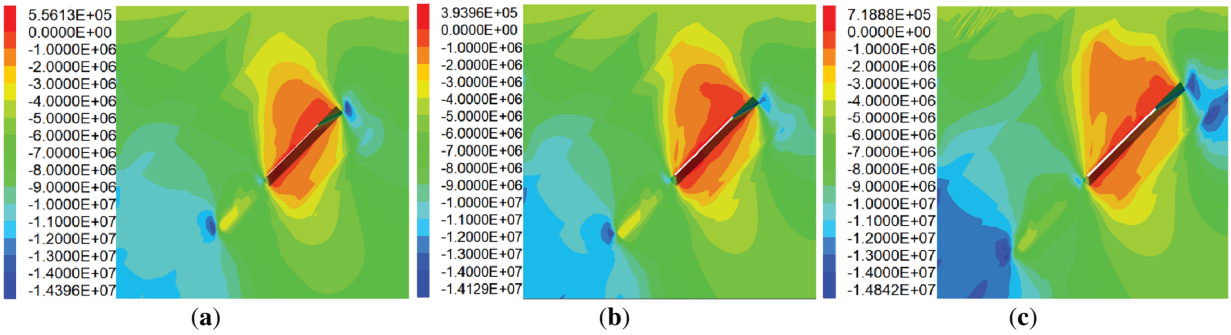

(**a**) (**b**) (**c**)

Figure 23: Vertical stress nephograms of overlying strata in steeply inclined coal seams under different working face length. (a) At 90 m working face length; (b) At 105 m working face length; (c) At 120 m working face length

Fig. 24 illustrates the stress monitoring profile of the roof under a constant backfill ratio across different working face lengths (90, 105, and 120 m). The results show that as the inclination length of the working face increases, the stress value at the lower-end coal pillar gradually rises to 13.27, 14.45, and 15.20 MPa, with increase rates of 8.89% and 5.19%, respectively. Furthermore, not only does the coal pillar stress progressively increase, but the strata behavior also exhibits significant differences. The 90 m working face shows intense but localized pressure concentration; the 105 m face demonstrates a double-peak characteristic with an expanded influence range and increasingly complex roof structure; at the 120 m long working face, pressure release becomes more gradual and sustained, highlighting the prominent role of the roof's macro-structure. This indicates that as the working face lengthens, strata behavior transitions from locally intense concentration to a broad, gradual release process.

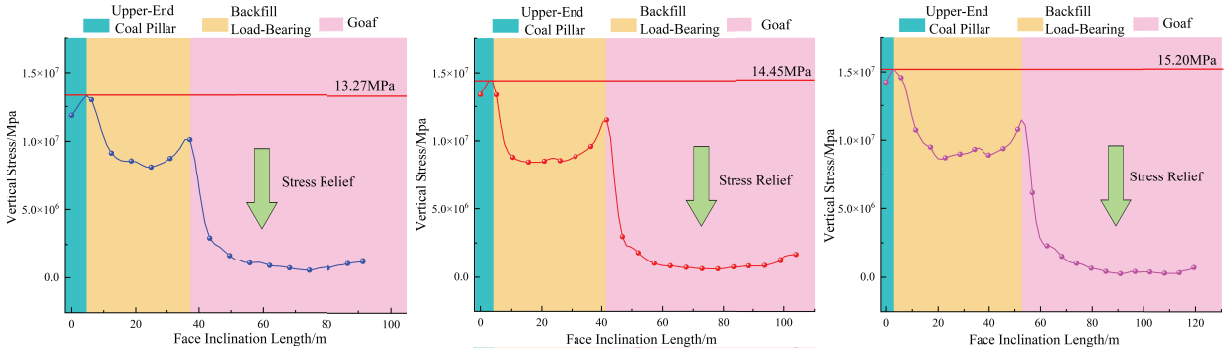

Figure 24: Vertical stress profiles of roof in steeply inclined coal seams under different working face length. (a) At 90 m working face length; (b) At 105 m working face length; (c) At 120 m working face length

(2) Displacement Distribution Characteristics of Overlying Strata

Under a constant backfill ratio of 2/5, vertical displacement nephograms were obtained under different working face inclination lengths, as shown in Fig. 25, the color gradient from red to blue in the figure not only represents the magnitude variation of displacement but also indicates its direction, where red denotes the positive direction (upward displacement) and blue signifies the negative direction (downward displacement), with units in meters (m). Analysis indicates that as the inclination length of the working face increases, the displacement field of the goaf roof progressively extends toward the top of the model, with the most pronounced displacement changes consistently observed in the middle-lower section of the goaf. This phenomenon occurs because, in steeply inclined working faces, an increase in face length directly leads to a greater load-bearing capacity requirement of the roof, which promotes the upward transmission of the bending deformation range into the upper overlying strata. Simultaneously, influenced by the coal seam dip angle, strata movement exhibits distinctly asymmetric characteristics, with the middle-lower section of the goaf becoming the concentration zone for displacement changes due to its location in the most complex stress state area.

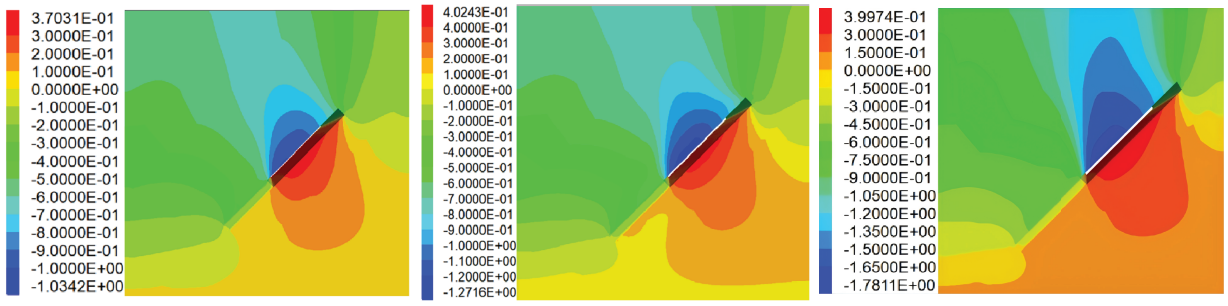

Figure 25: Vertical displacement nephograms of overlying strata in steeply inclined coal seams under different working face length. (a) At 90 m working face length; (b) At 105 m working face length; (c) At 120 m working face length

Fig. 26 presents the displacement monitoring profile of the roof under a constant backfill ratio across different working face lengths (90, 105, and 120 m). The results show that as the working face

length increases, the maximum vertical subsidence displacement of the roof grows from approximately 0.92 to 1.08 m and then to 1.61 m, representing increases of 17.4% and 49.1%, respectively, demonstrating a clear ascending trend. Under the same backfill ratio, the increase in working face length significantly expands the exposed area of the goaf, thereby enhancing the dead load of the overlying strata. This expansion of the unsupported roof span, coupled with the increased load, relatively weakens the self-bearing capacity of the roof structure. Concurrently, the enlarged goaf area and the increased overburden load cause the roof structure to gradually evolve from a "local cantilever" system to a "large-span beam-slab" system, significantly extending both the range and depth of its bending deformation.

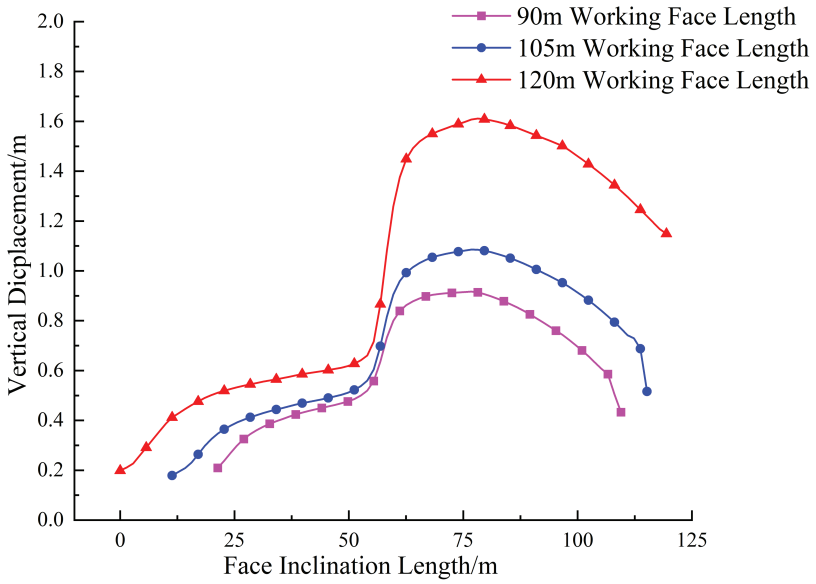

Figure 26: Vertical displacement profiles of roof in steeply inclined coal seams under different working face length

(3) Plastic Failure Characteristics of Overlying Strata

Under a constant backfill ratio of 2/5, failure nephograms of the model's plastic zone were obtained under different working face inclination lengths, as shown in Fig. 27. Analysis reveals that as the working face length increases, the development height of the failure zone in the overlying strata of the goaf continuously increases. When the working face inclination lengths are 90, 105, and 120 m, the development heights of the plastic zone in the overlying strata are 30.98, 36.05, and 65.56 m, with growth rates of 19.5% and 81.86%, respectively. This variation characteristic indicates that when the working face length increases beyond 105 m, the development of the plastic zone breaks through the confinement of the key strata, leading to a qualitative change in the failure mode. Specifically, the slow growth from 90 to 105 m reflects the effective utilization of the load-bearing capacity of the strata itself, while the sharp expansion of the plastic zone at 120 m suggests that the roof structure is approaching its bearing limit. This results in the complete disruption of the stress equilibrium within the strata, forming through-going failure.

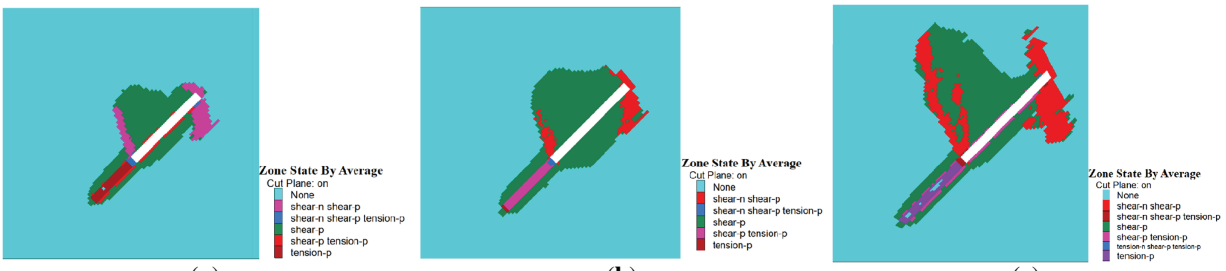

(**a**) (**b**) (**c**)

Figure 27: Failure characteristics of overlying strata in steeply inclined coal seams under different working face length. (a) At 90 m working face length; (b) At 105 m working face length; (c) At 120 m working face length

Based on a comparative analysis of stress, displacement, and plastic failure under a constant 2/5 backfill ratio, the 105 m working face length is determined to be optimal for steeply inclined coal seam mining. Stress distribution analysis shows that the 105 m length avoids the severe concentration seen at 120 m and the insufficient pressure relief of the 90 m face, forming a stable stress arch. In terms of displacement, roof subsidence increases controllably at 105 m, whereas extending to 120 m triggers a disproportionate surge in deformation. Most critically, plastic zone development reveals a stability threshold: growth remains gradual up to 105 m but escalates drastically beyond it, indicating a qualitative shift toward structural failure. Therefore, the 105 m length achieves the optimal balance between extraction efficiency and roof control, providing the most favorable engineering solution under the given conditions.

Integrating theoretical analysis, physical similarity simulation experiments, and the aforementioned numerical simulation results, it is concluded that an optimal and controllable outcome can be achieved under a working face length of 105 m and a backfill ratio of 2/5. Next, the progressive excavation process along the face strike in stages of 20, 40, 60, and 80 m will be simulated. The stress, displacement, and plastic zone evolution of the overlying strata at each advance stage will be comparatively analyzed to reveal the strata movement and strata behavior under the identified optimal parameters.

4.4 Result Analysis during Advance along the Strike under Optimal Parameters

(1) Stress Distribution Characteristics of Overlying Strata

Fig. 28 shows the stress contour maps of the immediate roof at advancement distances of 20, 40, 60, and 80 m. (To highlight the three-dimensional effect, the simulated stress values of the immediate roof stress contour maps were inverted. Therefore, compressive stresses are displayed as positive values, while tensile stresses are represented as negative values.)

In partially backfilled high-angle coal deposits, the surrounding strata exhibit dip-directional asymmetric evolution in their stress field configuration. The upper-middle section of the unfilled zone experiences stress relief through the combined effects of mining activity and backfill interaction, forming pressure-relief zones in both the upper-middle and central sections with an average stress reduction of 1.01 MPa. Simultaneously, clearly defined stress concentration areas emerge within flanking coal ribs at the roof and floor horizons, manifesting distinct peak stress differentials. The immediate roof registers average peak stresses of 9.74 (upper side) and 10.07 MPa (lower side), respectively. These asymmetric arch-shaped stress concentration areas exhibit more extensive influence

scope in the bottom region than in the top zone. Furthermore, the dip-direction upper-end coal pillars show elevated stress values relative to unfilled positions. However, due to the seam's inclination, the overburden loading on these upper-end pillars remains less than that acting on both lower-end pillars and the partial backfill zone.

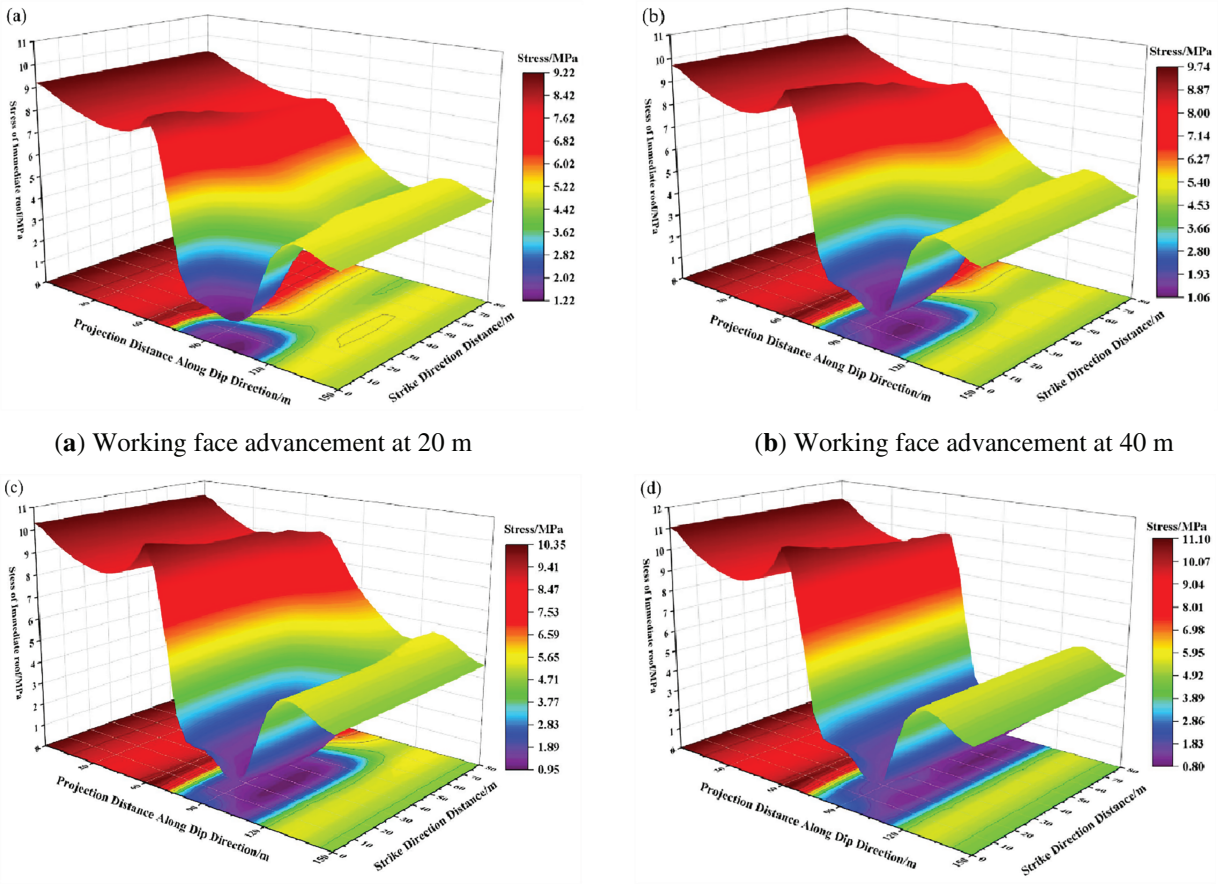

(**a**) Working face advancement at 20 m

(**b**) Working face advancement at 40 m

(**c**) Working face advancement at 60 m

(**d**) Working face advancement at 80 m

Figure 28: Stress contour map of immediate roof during mining

A pronounced stress concentration emerges proximal to the longwall face during strike-parallel extraction operations. The mining-induced overburden stress progressively shifts toward both the lower-end coal pillar and backfill body, inducing persistent abutment pressure increases along the coal-solid boundary in the lower extremity and backfill zones. This stress redistribution pattern clearly illustrates the dynamic load-transfer mechanism inherent to steeply inclined coal seam mining with partial backfilling. Quantitative measurements reveal systematic pressure variations at different advancement stages. The lower-end coal pillar shows peak abutment pressures of 9.22, 9.74, 10.35, and 11.10 MPa at 20, 40, 60, and 80 m advancement distances, respectively, accumulating a 20.4% total pressure increase. Similarly, the backfill body exhibits peak pressures of 8.75, 9.48, 10.11, and 10.91 MPa at corresponding distances, with a more pronounced 24.7% overall growth. In contrast, the upper-end coal pillar displays a distinctive "growth-stabilization" behavior, with maximum pressure values fluctuating moderately between 5.27 and 5.47 MPa throughout the advancement process.

(2) Displacement Distribution Characteristics of Overlying Strata

Fig. 29 shows the displacement contour maps of the immediate roof at advancement distances of 20, 40, 60, and 80 m.

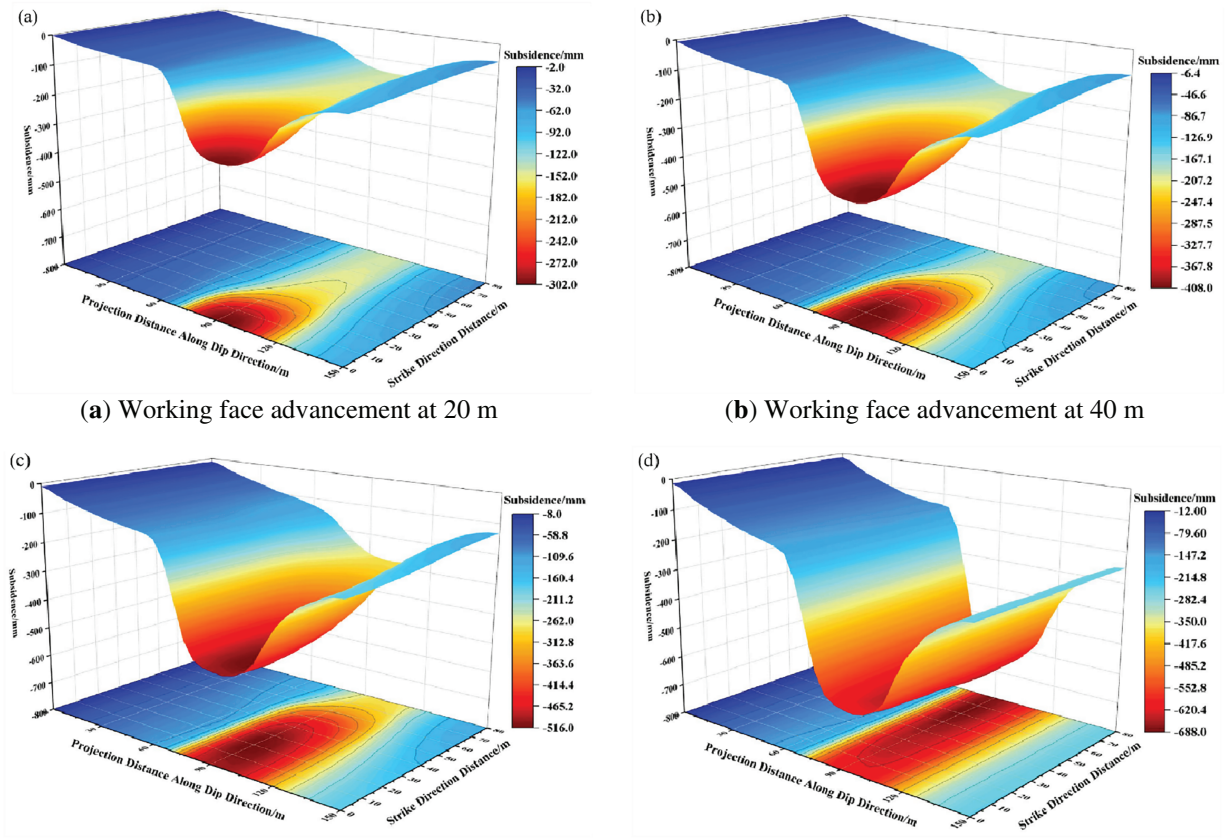

(**a**) Working face advancement at 20 m

(**b**) Working face advancement at 40 m

(**c**) Working face advancement at 60 m

(**d**) Working face advancement at 80 m

Figure 29: Displacement contour map of immediate roof during mining

Analysis of the figure indicates that progressive face advancement generates a characteristic "V-shaped" subsidence profile in the overburden displacement distribution along the face dip direction, with maximum subsidence occurring in the upper-middle section of the unfilled zone. Concurrently, the advance-induced strata movement along the face strike direction displays gradually increasing displacement magnitudes that extend deeper into the goaf area. Quantitative measurements show direct roof maximum subsidence values of 302, 408, 516, and 688 mm at advance distances of 20, 40, 60, and 80 m, respectively, with corresponding dip-direction advance distances measuring 91.2, 92.4, 91.8, and 91.5 m.

(3) Plastic Failure Characteristics of Overlying Strata

Figs. 30 and 31 show the plastic zone contour maps at advancement distances of 20, 40, 60, and 80 m.

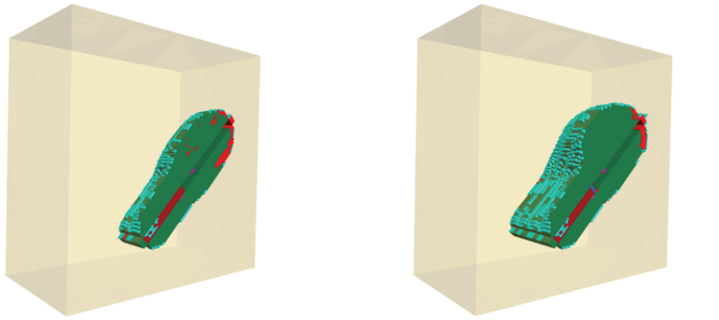

(**a**) Working face advancement at 20 m (**b**) Working face advancement at 40 m

(**c**) Working face advancement at 60 m (**d**) Working face advancement at 80 m

Figure 30: Damage localization phenomena in stope-overlying lithologic assemblies

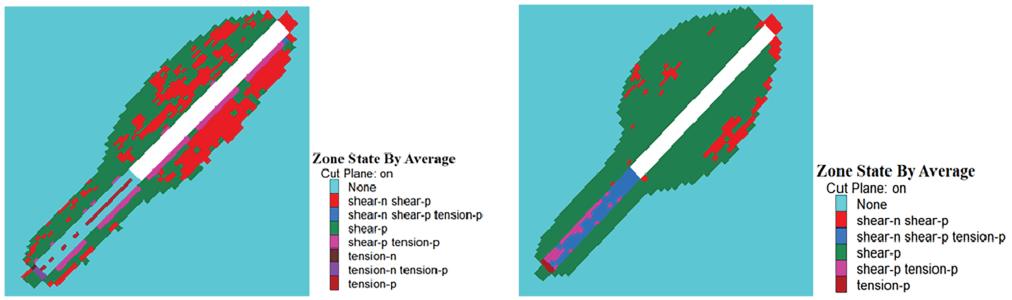

(**a**) Working face advancement at 20 m (**b**) Working face advancement at 40 m

(**c**) Working face advancement at 60 m (**d**) Working face advancement at 80 m

Figure 31: Damage localization phenomena in stope-overlying lithologic assemblies along dip direction of working face

Integrated analysis of Figs. 30 and 31 demonstrates that plastic zone development in both roof and floor strata progressively expands with face advance distance. The upper-middle roof section develops plastic zones first, predominantly through tensile failure. At 40 m advancement, the plastic zone extends toward both roof ends, forming an arched configuration with shear failure becoming dominant—indicating initial caving of the immediate roof in unfilled zones while the backfill experiences tensile principal stresses, with stable overburden plastic zone dimensions. When reaching 60 m advance, the unfilled roof's plastic zone abruptly expands vertically into the main roof layer, confirming main roof initial collapse. During this phase, the backfill undergoes shear-dominant principal stresses while the backfilled zone's plastic zone stabilizes, with roof failure scope substantially exceeding floor plastic zone development (demonstrating clear roof-floor asymmetry). At 80 m advance, the plastic zone further propagates into deeper strata with an asymmetric arch-shaped pattern, showing greater expansion in middle-lower regions. Simultaneously, roof shear failure intensifies at backfill-unfill interfaces, eventually penetrating the plastic zone's arch crown.

As the mining face advances, plastic failure in the coal seam roof and floor dynamically propagates three-dimensionally. Prior studies indicate that under identical crack dimensions and global strain conditions, CTOD (Crack Tip Opening Displacement) values increase in thicker-walled pipelines, with plastic deformation heavily influenced by internal pressure [33]. During mining operations, plastic failure within backfill materials evolves dynamically and expands spatially, where the morphology of plastic zone development directly manifests this three-dimensional transformation.

At the interface between backfilled and unfilled zones, partial backfill materials remain subjected to residual loads from the overlying unfilled strata. This region experiences elevated internal pressure and multi-directional compressive stresses, inducing strain-driven thickness reduction that amplifies plastic failure while reducing CTOD values. Conversely, the middle-lower sections of backfill bear diminished loads, exhibiting greater crack resistance with limited fracture development. Minimal or no plastic failure occurs in localized bottom areas due to reduced stress exposure.

These plastic zone characteristics verify that partial gangue backfill in steeply inclined seams effectively limits surrounding rock failure in unfilled zones through overlying backfill constraints. The backfilled area maintains minimal and stable plastic zone development, proving this method's efficacy in controlling roof failure and preserving surrounding rock structural stability.

Through numerical simulation, the trend of immediate roof displacement was analyzed. The results show that the maximum subsidence aligns with the physical experimental data, with the location of maximum displacement consistently observed in the mid-upper section of the unfilled area. Meanwhile, the trends in peak abutment stress at the lower end and the stress on the backfill body are also consistent with the physical experiments, both increasing progressively with mining advance, indicating a rising trend in the abutment stress of the lower-end coal pillar during continuous extraction. Thus, the numerical simulations and physical similarity experiments corroborate each other, jointly establishing the reliability and scientific validity of the overburden response mechanisms under local backfill control.

5 Conclusions

This study investigates deformation mechanisms in superjacent strata and geotechnical stabilization measures for peripheral rock formations within high-inclination coal deposits employing zonal gob backfill. Significant outcomes demonstrate:

(1) Within steep coal seams employing partial gangue backfill, four predominant factors control roof deformation and failure mechanisms: working face length, mining depth, seam inclination angle, and backfill body length. Comprehensive analysis reveals that roof rotation angle, deflection values, and bending moments increase proportionally with working face length and mining depth, yet decrease with greater coal seam dip angles and extended backfill lengths. Significantly, the investigation establishes that optimal roof stability control is achieved when the backfill length constitutes 40% of the total working face length (equivalent to two-fifths coverage).

(2) In steeply dipping coal seams utilizing partial gangue backfilling, the collapsed waste rock in the goaf area demonstrates significant non-uniform filling characteristics, with pronounced spatial heterogeneity in both compaction density and stress distribution along the dip direction. As face advancement progresses, the main roof in unfilled zones undergoes initial caving, while the fragmented gangue in deeper goaf regions develops a distinct stratified architecture characterized by: high-density compaction in basal layers, intermediate compaction in medial strata, and relatively loose accumulation in upper sections. Conversely, the surrounding rock mass within backfilled zones maintains remarkable overall stability, with its displacement evolution following a well-defined three-stage pattern: initial stabilization, progressive increase, and eventual re-stabilization. Therefore, local gangue filling can effectively control the stability of roof in working face.

(3) Using a controlled variable approach, the overlying strata movement, strata behavior, and plastic failure characteristics were analyzed by varying the backfill ratio and working face length, respectively. The results indicate that optimal overlying strata control and ideal mining conditions are achieved under a working face length of 105 m and a backfill ratio of 2/5. At this backfill ratio, roof stress concentration is effectively mitigated, strata displacement increases steadily, and a stable asymmetric plastic arch structure can form. Building upon this backfill condition, the 105 m working face length further ensures balanced stress distribution, controllable displacement variation, and moderate plastic zone development, thereby avoiding the insufficient pressure relief observed under the 90 m condition and the risk of through-going plastic failure under the 120 m condition.

(4) Computational modeling reveals distinct stress reconfiguration parallel to the seam dip, with significant stress concentrations developing at critical zones: the foundation level of the inferior pillar and the central domain of the backfill segment. Concurrently, stress relief develops preferentially in the upper-middle section of the unfilled zone, exhibiting more pronounced effects compared to the central area. This asymmetric stress evolution establishes a coupled "concentration-release" mechanism that fundamentally governs roof behavior and ground pressure dynamics in this mining configuration. The overburden displacement displays a characteristic "V-shaped" subsidence profile along the dip direction, with subsidence magnitudes following a consistent spatial sequence: unfilled zone (maximum) > upper-end coal pillar > backfilled zone > lower-end coal pillar (minimum). Mechanistically, the shear failure zones are primarily distributed in the stress concentration areas near the arch foot, especially around the lower-end coal pillar and the interface with the backfill body along the dip direction. These regions form high shear stress zones due to stress concentration and serve as key supporting parts for maintaining the mechanical equilibrium of the arch structure. In contrast, the tensile failure zones mainly occur in the arch crown and pressure relief areas, reflecting the tensile cracks generated by the bending deformation of the overlying strata, which correspond to the separation and pressure release within the arch shell. The asymmetric distribution of

these two failure modes along the dip direction visually demonstrates the geometric and mechanical asymmetry of the stress arch shell under steeply dipping coal seam conditions, further validating the formation, evolution, and controlling role of the overburden stress arch shell in partial backfill mining.

6 Discussion

(1) In this study, the physical similarity simulation experiment in Section 3 and the FLAC3D numerical simulation in Section 4 collectively reveal, at a macroscopic level, the core mechanisms of asymmetric deformation, stress-arch evolution, and the controlling effect of the backfill in steeply inclined coal seams under partial backfill mining. The conclusions drawn from the two approaches are mutually corroborative. However, there exist minor, explainable discrepancies in the specific stress and displacement values as well as local evolutionary details, primarily stemming from the fundamental differences between the two research methodologies. The physical experiment employs similar materials whose mechanical behavior meets similarity criteria macroscopically but exhibits heterogeneity microscopically. Furthermore, the experimental process can realistically reproduce discontinuous and nonlinear physical phenomena such as strata separation, fracturing, collapse, and the sliding accumulation of gangue. Consequently, the monitored abutment pressure peaks are higher, and the displacement evolution exhibits a phased "stable–surge–stable" characteristic associated with collapse events. In contrast, the numerical simulation is based on continuum mechanics and idealized elasto-plastic constitutive models. Its computational results are approximate solutions of theoretical equations under given parameters, leading to a more continuous and smooth output stress field and a more linear displacement growth trend. It struggles to fully capture the instantaneous mutations and complex rock block structures during actual failure processes. These differences do not represent contradictions; instead, they highlight the respective strengths of each method. The physical experiment offers an intuitive advantage in replicating the physical phenomena that occur in actual geotechnical engineering contexts, while the numerical simulation provides a theoretical advantage in delivering full-field, continuous data and enabling parametric analysis. The combination of the two precisely constitutes a methodological cross-validation and complementarity, fully demonstrating the robustness and scientific rigor of the conclusions drawn in this study.

(2) After employing a three-dimensional physical similarity simulation experiment to reveal the strata behavior patterns, overburden movement characteristics, and failure morphology in steeply inclined coal seams under partial backfill mining, this study also recognizes the inherent limitations of the model. Firstly, although the similar materials used in the experiment meet the similarity criteria in terms of macroscopic mechanical parameters such as bulk density and strength, their homogeneous and continuous nature cannot fully replicate the complex heterogeneity, anisotropy, and joint-fracture distribution of *in-situ* rock masses. This may lead to more regular and continuous fracture patterns in the model strata. Secondly, the scaled model based on a fixed geometric similarity ratio (1:100) inevitably introduces scale effects, making it difficult to fully equivalently simulate certain mesoscopic processes important in the prototype, such as the interlocking effect between rock blocks and time-dependent rheological behavior. Therefore, the quantitative data obtained from the experiment need to be converted using the similarity ratio and calibrated against field data. However, the core trends and relative patterns revealed possess clear physical significance and mechanistic universality. The primary objective of this experiment is to qualitatively uncover the key mechanisms and spatial

patterns of overburden response under complex steeply inclined conditions, providing a reliable validation benchmark for theoretical models and numerical simulations. When applying its conclusions to specific engineering practices, comprehensive analysis considering the specific geological and mining conditions is required.

(3) In the numerical simulation section, this study constructed a computational model based on a series of necessary and reasonable simplifying assumptions. While these assumptions ensured computational feasibility, they also introduced certain limitations. Firstly, the model adopts the Mohr-Coulomb elastoplastic constitutive model and assumes linear elastic behavior of materials before yielding. Although this approach effectively determines shear and tensile failure, it cannot describe post-peak behaviors such as strain softening, anisotropy, and time-dependent rheological effects in rock masses. Secondly, treating all rock layers and backfill materials as homogeneous, continuous, and isotropic media overlooks the actual heterogeneity, joints, and bedding structures of rock masses. This may lead to idealized stress transmission and failure patterns in the simulation compared to real conditions. Lastly, the model employs uniformly distributed equivalent loads and simplified boundary constraints, without considering the influence of complex *in-situ* stress fields, which may affect the accuracy of the local morphology and absolute values of the stress arch shell. Despite these simplifications, they did not hinder the effective revelation of the movement patterns of the overburden, the manifestation of strata behavior, and the failure conditions of surrounding rock under partial backfill conditions. The obtained results correspond with and validate the conclusions from physical experiments and theoretical analyses, demonstrating the scientific rigor and credibility of this study.

(4) The study indicates that implementing partial waste rock backfill mining is crucial in areas with steep coal seam dip angles. In practical engineering, this translates into a well-defined design framework: first, the working face length is set at approximately 105 m based on geological and equipment conditions, followed by high-quality waste rock backfilling prioritized within the lower 40 m section of the working face. This design ensures the formation of a stable stress-bearing core at the lower-end coal pillar and the central part of the backfill body, thereby actively transferring overburden pressure to this controllable zone and effectively preventing disordered stress concentration in the middle-upper section of the roof. With the field application of this scheme, it is expected that the location of maximum roof subsidence will stabilize in the upper-middle part of the unfilled zone, with subsidence significantly controlled. Meanwhile, the support pressure in the lower-end roadway will increase but tend to stabilize rather than fluctuate sharply, greatly reducing the risk of rock burst. More importantly, the overburden will spontaneously form an asymmetric "stress-arch shell" structure, with its "arch foot" located in the backfill area and the lower-end coal pillar, and its "arch crown" situated above the unfilled zone. This structure can effectively bear the weight of the overlying strata over the long term. Therefore, the key to engineering implementation lies in ensuring the strength and stability of the lower-end coal pillar, as well as the initial compaction density and roof-contact effectiveness of the backfill material. The monitoring system should be focused on the upper-middle roof of the unfilled zone and the lower-end roadway.

Acknowledgement: Not applicable.

Funding Statement: This work was supported by the National Natural Science Foundation of China (No. 52174127, 52374137), the Youth Innovation Team Project of Shaanxi University, and the Outstanding Youth Science Fund Project of Shaanxi (2023-JC-JQ-42).

Author Contributions: All authors contributed to the study conception and design. Material preparation, data collection and analysis were performed by Wenyu Lv, Jinghui Wang, Chao Lyu, Yongping Wu, Panshi Xie, Xuyan He, Kai Guo and Ru You. The first draft of the manuscript was written by Jinghui Wang and all authors commented on previous versions of the manuscript. All authors reviewed and approved the final version of the manuscript.

Availability of Data and Materials: Data available on request from the authors.

Ethics Approval: Not applicable.

Conflicts of Interest: The authors declare no conflicts of interest.

References

1. Zhang L, Luo L, Pan J, Li X, Sun W, Tian S. Seepage characteristics of coal under complex mining stress environment conditions. Energy Fuels. 2024;38(17):16371–84.
2. Wang F. Formation mechanism of high-cold and high-altitude landslide disasters caused by complex goaf groups. J Min Sci. 2025;61(1):71–9. doi:10.1134/S1062739125010077.
3. Wu YP, Yun DF, Xie PS, Wang HW, Lang D, Hu BS. Progress, practice and scientific issues in steeply dipping coal seams fully-mechanized mining. J China Coal Soc. 2020;45(1):24–34. (In Chinese). doi:10.13225/j.cnki.jccs.YG19.0494.
4. Fu Q, Yang K, Wei Z, He X. Study on ultimate strength and dip effect of coal pillar in steeply dipping coal seam. Geotech Geol Eng. 2023;41(6):3447–57. doi:10.1007/s10706-023-02467-9.
5. Wei Z, Yang K, Chi X, Liu W, Zhao X. Dip angle effect on the main roof first fracture and instability in a fully-mechanized workface of steeply dipping coal seams. Shock Vib. 2021;2021(1):5557107. doi:10.1155/2021/5557107.
6. Zhang YX, Wang K. Roof broken features at fully mechanized caving mining stope in steep inclined and specially thick seam. Saf Coal Mines. 2014;45(7):187–91. (In Chinese). doi:10.13347/j.cnki.mkaq.2014.07.056.
7. Yin W, Bai X, Wu J, Zhang R, Liu C, Zhang R, et al. Mechanical analysis of basic roof fracture mechanism and feature in coal mining with partial gangue backfilling. Open Geosci. 2020;12(1):904–18. doi:10.1515/geo-2020-0153.
8. Zhao T. Ground control in mining steeply dipping coal seams by backfilling with waste rock. J South Afr Inst Min Metall. 2018;118(1):15–26. doi:10.17159/2411-9717/2018/v118n1a3.
9. Huang Y, Zhang J, Yin W, Sun Q. Analysis of overlying strata movement and behaviors in caving and solid backfilling mixed coal mining. Energies. 2017;10(7):1057. doi:10.3390/en10071057.
10. Zhen E, Dong S, Huang J, Wang Y, Wang M, Zhang X, et al. Analysis of the EFARC non-pillar mining stope: roof failure and overlying pressure in inclined coal seams. Geomech Geophys Geo Energy Geo Resour. 2023;9(1):151. doi:10.1007/s40948-023-00691-4.
11. Yin Y, Zou J, Zhang Y, Qiu Y, Fang K, Huang D. Experimental study of the movement of backfilling gangues for goaf in steeply inclined coal seams. Arab J Geosci. 2018;11(12):318. doi:10.1007/s12517-018-3686-0.
12. Yang K, He X, Liu S, Lu W. Rib spalling mechanism and control with fully mechanized longwall mining in large inclination three-soft thick coal seam under closed distance mined gob. J Min Saf Eng. 2016;33:611–7. (In Chinese). doi:10.13545/j.cnki.jmse.2016.04.007.
13. Zhang B, Cao S. Study on first caving fracture mechanism of overlying roof rock in steep thick coal seam. Int J Min Sci Technol. 2015;25(1):133–8. doi:10.1016/j.ijmst.2014.11.013.

14. Chi X, Yang K, Wei Z. Breaking and mining-induced stress evolution of overlying strata in the working face of a steeply dipping coal seam. Int J Coal Sci Technol. 2021;8(4):614–25. doi:10.1007/s40789-020-00392-3.
15. Zhang H, Hu G, Zhao G. Research on the movement law of roof structure in large-inclined coal seam working face: a case study in Liu.Pan.Shui. mining area. Shock Vib. 2022;2022(1):6328851. doi:10.1155/2022/6328851.
16. Wang Y, Wang Q, Tian X, Wang H, Yang J, He M. Stress and deformation evolution characteristics of gob-side entry retained by roof cutting and pressure relief. Tunn Undergr Space Technol. 2022;123:104419. doi:10.1016/j.tust.2022.104419.
17. Wang M, Li X, Su J, Liu W, Fang Z, Wang S, et al. A study on the reasonable width of narrow coal pillars in the section of hard primary roof hewing along the air excavation roadway. Energy Sci Eng. 2024;12(6):2746–65. doi:10.1002/ese3.1799.
18. Huang L, Guan W, Guan Y, Zhao H, Zhang Z, Wen Y. Overburden movement law in strip filling mining of upward mining faces. Sci Rep. 2025;15(1):1378. doi:10.1038/s41598-024-82930-6.
19. Kong DZ, Xiong Y, Cheng ZB, Wang N, Wu GY, Liu Y. Stability analysis of coal face based on coal face-support-roof system in steeply inclined coal seam. Geomech Eng. 2021;25:233–43. doi:10.12989/gae.2021.25.3.233.
20. Ma LQ, Zhang Y, Zhang DS, Cao XQ, Li QQ, Zhang YB. Support stability mechanism in a coal face with large angles in both strike and dip. J South Afr Inst Min Metall. 2015;115(7):599–606. doi:10.17159/2411-9717/2015/v115n7a6.
21. Wang JA, Jiao JL. Criteria of support stability in mining of steeply inclined thick coal seam. Int J Rock Mech Min Sci. 2016;82:22–35. doi:10.1016/j.ijrmms.2015.11.008.
22. Yang SL, Zhao B, Li LH. Coal wall failure mechanism of longwall working face with false dip in steep coal seam. J China Coal Soc. 2019;44(2):367–76. (In Chinese). doi:10.13225/j.cnki.jccs.2018.1380.
23. Li J, Yan B, Dong J, Qiang X, Chen C, Zhou G, et al. Analysis of main roof mechanical state in inclined coal seams with roof cutting and gob-side entry retaining. Symmetry. 2025;17(5):723. doi:10.3390/sym17050723.
24. Deng Y, Wang S. Feasibility analysis of gob-side entry retaining on a working face in a steep coal seam. Int J Min Sci Technol. 2014;24(4):499–503. doi:10.1016/j.ijmst.2014.05.013.
25. Yin Y, Chen J, Zhao Z, Yang Y, Li C, Li H, et al. Integrated geophysical prospecting for deep ore detection in the Yongxin gold mining area, Heilongjiang. China Sci Rep. 2025;15(1):7258. doi:10.1038/s41598-025-92108-3.
26. Wang M, Fang Z, Li X, Kang J, Wei Y, Wang S, et al. Research on the prediction method of 3D surface deformation in filling mining based on InSAR-IPIM. Energy Sci Eng. 2025;13(5):2401–14. doi:10.1002/ese3.70040.
27. Wang JA, Jiao JL, Cheng WD, Yun DF, Xie JW, Shangguan KF. Roles of arc segment in controlling the support stability in longwall fully mechanized top coal caving mining face of steeply inclined coal seam. J China Coal Soc. 2015;40:2361–9. (In Chinese). doi:10.13225/j.cnki.jccs.2015.0036.
28. Cui F, Lei Z, Chen J, Chang B, Yang Y, Li C, et al. Research on reducing mining-induced disasters by filling in steeply inclined thick coal seams. Sustainability. 2019;11(20):5082. doi:10.3390/su11205802.
29. Tu HS, Tu SH, Fang C, Chen WA, Feng YF. Study on the deformation and fracture feature of steep inclined coal seam roof based on the theory of thin plates. J Min Saf Eng. 2014;31(1):49.
30. Zhou H, Liu Z, Shen W, Feng T, Zhang G. Mechanical property and thermal degradation mechanism of granite in thermal-mechanical coupled triaxial compression. Int J Rock Mech Min Sci. 2022;160(5):105270. doi:10.1016/j.ijrmms.2022.105270.
31. Hu K, Liu B, Pang Y, Li R, Zhang Q, Shi J, et al. H_2 and CH_4 adsorption on coal: insights from experiment and mathematical model. Int J Hydrogen Energy. 2025;120:542–57. doi:10.1016/j.ijhydene.2025.03.233.

32. Wang H, Wu Y, Liu M, Jiao J, Luo S. Roof-breaking mechanism and stress-evolution characteristics in partial backfill mining of steeply inclined seams. Geomat Nat Hazards Risk. 2020;11(1):2006–35. doi:10.1080/19475705.2020.1823491.
33. Zhang YM, Xiao ZM, Zhang WG, Huang ZH. Strain-based CTOD estimation formulations for fracture assessment of offshore pipelines subjected to large plastic deformation. Ocean Eng. 2014;91:64–72. doi:10.1016/j.oceaneng.2014.08.020.